

3-manifolds algorithmically bound 4-manifolds

by

Samuel Churchill

B.Sc., University of Victoria, 2013

A Thesis Submitted in Partial Fulfillment of the
Requirements for the Degree of

Master of Science

in the Department of Mathematics and Statistics

© Samuel Churchill, 2019

University of Victoria

All rights reserved. This dissertation may not be reproduced in whole or in part, by
photocopying or other means, without the permission of the author.

3-manifolds algorithmically bound 4-manifolds

by

Samuel Churchill

B.Sc., University of Victoria, 2013

Supervisory Committee

Dr. Ryan Budney, Supervisor
(Department of Mathematics and Statistics)

Dr. Heath Emerson, Departmental Member
(Department of Mathematics and Statistics)

Dr. Alan Mehlenbacher, Outside Member
(Department of Economics)

Contents

Supervisory Committee	ii
Table of Contents	iii
List of Figures	iv
1 Introduction	1
1.1 Expected Background	2
1.2 Agenda	2
2 Tools of low-dimensional topology	3
2.1 Handles	3
2.2 Stratification	4
2.3 Handlebodies	5
3 Construction for smooth manifolds	8
3.1 Projections from 3-manifolds to \mathbb{R}^2	9
3.2 Stratifying \mathbb{R}^2	10
3.3 Stratifying M	14
3.4 Attach Handles	23
4 Algorithm for triangulated manifolds	30
4.1 Define projection	31
4.2 Induce subdivision	33
4.3 Attach Handles	37
5 Discussion	43
Bibliography	45

List of Figures

2.1	Genus 1 Heegaard splitting of S^3. The purple curve is essential in each solid torus pictured. In the left torus it is a meridian, on the right a longitude.	7
3.1	Forming vertex regions. Octagonal sleeves are fit around codimension 2 singular values to form vertex regions. Codimension 1 singular values are illustrated in black and their crossings, codimension 2 singular values, are indicated in red. Note that the edges of the octagonal sleeves alternate between containing exactly one singular value, its intersection with a black arc, or consisting entirely of regular values. New vertex regions are shaded orange.	11
3.2	Forming edge regions. Vertex region corners are connected to fit sleeves around arcs of codimension 1 singular values to form edge regions. New edge regions are shaded blue.	12
3.3	Forming face regions. All remaining regions contain no singular values, and we take these to be the face regions. New face regions are shaded green.	13
3.4	Connected singular fibers. List of connected singular fibers of proper C^∞ stable maps of orientable 3-manifolds into surfaces. κ is the codimension of the singularity in the surface. The singular fiber above a codimension 2 singular value may be disconnected, in which case the fiber is the disjoint union of a pair of singular fibers from $\kappa = 1$	16
3.5	Surfaces over codimension 1 singularities. γ_s is an arc of singular values and γ_t is an arc with endpoints $\partial\gamma_t = \{p, q\}$ that intersects γ_s transversely at $x = \gamma_s \cap \gamma_t$. The three surfaces shown are the three possible cross-sectional surfaces that can project through f over γ_t	18

3.6	Definite and indefinite blocks. The blocks containing sections of definite and indefinite folds that project over codimension 1 singular values. These are found as singular fibers over edge and vertex regions.	19
3.7	Resolutions of the singular points in the first interactive fiber. The singular fiber inside of B_x and its possible resolutions over nearby codimension 1 singular values and regular values. The fibers inherit orientation from M , and this illustration is presented without loss of generality. This figure is modeled after Figure 18 from [3].	20
3.8	Surface Σ near the first interactive fiber that projects over $\partial\bar{\nu}(x)$. The surface and B_x are presented as embedded in S^3 , where $H(B_x)$ is the genus-3 (3,1)–handlebody on the ‘inside’ of Σ in S^3 .	21
3.9	Resolutions of the singular points in the second interactive fiber. The singular fiber inside of B_x and its possible resolutions over nearby codimension 1 singular values and regular values. The fibers inherit orientation from M , and this illustration is presented without loss of generality. This figure is modeled after Figure 16 from [3].	22
3.10	Surface Σ near the second interactive fiber that projects over $\partial\bar{\nu}(x)$. The surface and B_x are presented as embedded in S^3 , where $H(B_x)$ is the genus-3 (3,1)–handlebody on the ‘outside’ of Σ in S^3 .	23
3.11	A face block and its complement form S^3. A face block B is a stratified closed solid torus that is stratified-homeomorphic to $S^1 \times G_n$ for some n –gon G_n . The complement of its unknotted interior in S^3 is another stratified closed solid torus B' . B and B' are depicted as cylinders with top and bottom identified.	24
3.12	Edge blocks. The possible edge blocks of M_1 . Annular boundary strata that are incident with face blocks of M_1 are indicated in purple. For each block, attaching (3,2)–handles over the indicated annuli results in a stratified 3–manifold homeomorphic to $S^2 \times [0, 1]$.	26
3.13	The effect of stratified (4,2)–handle attachment on an example edge block. An edge block E , a face block complement B' , and the result of attaching $C(S_B^3)$ to W over B on E . The boundary stratum shared by E and B in M_1 is indicated in green, as is the corresponding boundary stratum of B' in S_B^3 .	26

3.14	Vertex block with (3,2)–handle attachment sites indicated. We display an example vertex block of M_1 . Recall that this is the second type of interactive vertex block and, as in Figure 3.10, the surface is presented as embedded in S^3 and the block is the stratified (3,1)–handlebody on the ‘outside’ of the surface in S^3 . Annular boundary strata that are incident with face blocks of M_1 are indicated in color and correspond to the shared vertex-face region boundary edge. The 1–handle belt spheres are also indicated as black horizontal arcs across the surface. Attaching (3,2)–handles over the indicated annuli as prescribed results in a (3,2)–handlebody.	28
4.1	A tetrahedron σ projected to the plane in standard position through a subdividing map f. The four vertices of σ^0 map to the unit circle in the plane, thus form a convex arrangement. Four of the six edge of σ^1 map to the boundary of $f(\sigma)$, connecting $f(\sigma^0)$. The last two edges map across $f(\sigma)$, forming an intersection interior to $f(\sigma)$. Each vertex of the arrangement is essential in forming the convex hull of $f(\sigma^0)$	33
4.2	A tetrahedron σ in standard position, intersecting edges, and preimage triangles and quads. An intersecting edge separates the vertices of σ . If one is separated from the other three, its preimage is a triangle. If the vertices are separated into two pairs of two, the preimage is a quad.	34
4.3	A tetrahedron σ in standard position, one interior triangle, one exterior triangle, and one exterior quad. There are two special preimage triangles in σ , called <i>interior triangles</i> , that occur as the preimages of the edges of σ that map through f across $f(\sigma)$ as in Figure 4.1.	34
4.4	A tetrahedron σ in standard position with both interior triangles. As in Figure 4.3, but displaying both interior triangles. . .	35
4.5	A pair of sleeve segments in the plane. We show a pair of edges projections $f(e)$ and $f(g)$ in the plane, along with their associated sleeve segments. Sleeve segments are necessary to ensure well-defined face, edge, and vertex block analogues in the subdivision of N	36

4.6	Regions in the plane that correspond to combinatorial vertex, edge, and face block. The sleeve segments provide the same functionality as the sleeves in Chapter 3, in that the preimages of the regions they form behave similarly to the vertex, edge, and face blocks defined in Chapter 3.	37
-----	---	----

Chapter 1

Introduction

The study of manifold boundaries is asymmetric. Given an n -manifold, it is trivial to find its unique $(n - 1)$ -manifold boundary. Given an $(n - 1)$ -manifold boundary, there are infinitely many n -manifolds that possess it but no obvious way to acquire one. We focus on the low-dimensional case of $n = 4$, where it is known that all closed, orientable 3-manifolds bound 4-manifolds (See [8, 10, 13] for a variety of approaches on this subject). The main goal of this document is to provide an algorithm that constructs 4-manifolds with a given boundary.

This century has seen the rise of computational means of constructing and studying low-dimensional manifolds using software such as Regina [1] and SnapPy [4]. The algorithm provided in this document is intended for eventual inclusion in Regina, where it will serve as a new tool for constructing 4-manifold censuses and studying 3-manifold invariants.

Our assemblage of a constructive proof that 3-manifolds bound 4-manifolds was inspired by the discussion in Section 2.2 of Costantino & Thurston’s “3-manifolds efficiently bound 4-manifolds” [3]. An appropriately well-behaved smooth map from a 3-manifold M to \mathbb{R}^2 induces a stratification of M into a union of handlebodies. This stratification serves as a set of surgery instructions for turning M into S^3 . It can also be interpreted as a set of 4-dimensional handle attachment sites, and attaching these handles to one boundary component of $M \times [0, 1]$ produces a 4-manifold whose boundary is precisely M .

Our algorithm is the adaptation of this smooth proof to the setting of triangulated manifolds. We define a map from the input 3-manifold triangulation to \mathbb{R}^2 , subdivide the manifold into handlebodies, then attach handles to one boundary component the manifolds’ 4-thickening until we obtain the desired outcome.

1.1 Expected Background

This document is aimed at a reader with some understanding of the tools of low-dimensional manifold theory. We do not present the basics of manifold theory, calculus on manifolds, or triangulations of manifolds.

For the fundamentals of manifolds and calculus on manifolds see Lee’s “Introduction to Smooth Manifolds” [6]. For more on 3-manifolds and an introduction to triangulations, see Stein, Thurston, & Mather’s “Three-dimensional geometry and topology” [?].

1.2 Agenda

What follows is a brief summary of the contents of each chapter in this document. Each chapter has a purpose, and that purpose is also stated.

Chapter 1 lays out what the central thesis problem is and why it is interesting. It also sets expectations for the rest of the document in terms of what to expect and what not to expect.

Chapter 2 presents some specialized tools of low-dimensional topology that are utilized throughout the document. It serves as a reference or refresher depending on the reader’s familiarity with the subject.

Chapter 3 presents the constructive proof in the smooth case. It fills a void in the current literature and anchors the abstraction of Chapter 4 to something accessible and visual.

Chapter 4 provides the main result of this document: the algorithm itself. It is a precursor to an implementation of the algorithm in a low-dimensional topology software package.

Chapter 5 restates our results and delves into implications on future work. It, along with Chapter 1 and the Abstract, provide an overview of the entirety of the document.

Chapter 2

Tools of low-dimensional topology

Given a smooth, closed 3-manifold M , there are infinitely many 4-manifolds with boundary M . For example, consider $M = S^3$. Removing a 4-ball from any 4-manifold W produces a 4-manifold with S^3 boundary. We therefore do not ensure that the constructed 4-manifold has any properties other than a specified boundary, so our construction prioritizes easy verification that the constructed 4-manifold's boundary is exactly M . This is done by setting $W = M \times [0, 1]$, so W has boundary

$$\partial W = (M \times \{0\}) \cup (M \times \{1\}) = M_0 \cup M_1.$$

We then attach stratified handles to the boundary of W away from M_0 until only M_0 remains.

2.1 Handles

The concept of a stratified handle attachment needs some explanation. First, we define attachment of topological spaces, and use that language to define handle attachment. We use Gompf & Stipsicz's "4-Manifolds and Kirby Calculus" [5] as our main reference for handle attachment.

Definition 2.1.1 (Attachment). Let X and Y be topological spaces, $A \subset X$ a subspace, and $f : A \rightarrow Y$ a continuous map. We define a relation \sim by putting $f(x) \sim x$ for every x in A . Denote the quotient space $X \sqcup Y / \sim$ by $X \cup_f Y$. We call the map f the *attaching map*. We say that X is *attached* or *glued* to Y over A . A space obtained through attachment is called an *adjunction space* or *attachment space*.

Alternatively, we let A be a topological space and let $i_X : A \rightarrow X$, $i_Y : A \rightarrow Y$ be inclusions. Here, the adjunction is formed by taking $i_X(a) \sim i_Y(a)$ for every $a \in A$ and we denote the adjunction space by $X \cup_A Y$.

Definition 2.1.2 (Handle). Take $n = \lambda + \mu$ and M a smooth n -manifold with nonempty boundary ∂M . Let D^λ be the closed λ -disk and put $H^\lambda = D^\lambda \times D^\mu$. Let $\varphi : \partial D^\lambda \times D^\mu \rightarrow \partial M$ be an embedding and an attaching map between M and H^λ . The attached space H^λ is an n -dimensional λ -handle, abbreviated (n, λ) -handle, and $M \cup_\varphi H^\lambda$ is the result of an n -dimensional λ -handle attachment, abbreviated (n, λ) -handle attachment.

Let $n = \lambda + \mu$, let $H^\lambda = D^\lambda \times D^\mu$ be a (n, λ) -handle, and let $\varphi : \partial D^\lambda \times D^\mu \rightarrow \partial M$ be an attaching map from H^λ to the n -manifold M . The sphere $\partial D^\lambda \times \{0\}$ in H^λ is the *attaching sphere* of H^λ , and the sphere $\{0\} \times \partial D^\mu$ is the *belt sphere* of H^λ .

Handles H_1 and H_2 attached to M are extraneous when $(M \cup H_1) \cup H_2 \approx M$. When this happens, we say that the handles *cancel*. In the proof of Theorem 3.4.1 we attach 2-handles with the intention of canceling 1-handles.

Proposition 2.1.3 (Proposition 4.2.9 in [5]). A $(k-1)$ -handle H^{k-1} and a k -handle H^k ($1 \leq k \leq n$) can be canceled, provided the attaching sphere of H^k intersects the belt sphere of H^{k-1} transversely in a single point.

Handle attachment is defined for smooth manifolds, but the resulting attachment space is not a smooth manifold. Rather, the result is a manifold with corners. Some other formulations of handle attachment (e.g. [5]) implicitly smooth the corners resulting from handle attachment, so in their formulation of handle cancellation the equivalence relation is strong (i.e. \approx is diffeomorphism). Instead of smoothing corners, we keep everything in the language of stratified spaces (introduced in Section 2.2). We therefore take \approx to be homeomorphism for the purposes of handle cancellation.

2.2 Stratification

We use Weinberger's "The topological classification of stratified spaces" [15] as our main reference for stratified spaces.

Definition 2.2.1 (Stratification). X is a *filtered space* on a finite partially ordered indexing set S if

1. there is a closed subset X_s for each $s \in S$,
2. $s \leq s'$ implies that $X_s \subset X_{s'}$, and
3. the inclusions $X_s \hookrightarrow X_{s'}$ satisfy the homotopy lifting property.

The X_s are the *closed strata* of X , and the differences

$$X^s = X_s \setminus \bigcup_{r < s} X_r$$

are *pure strata*.

A *filtered map* between spaces filtered over the same indexing set is a continuous function $f : X \rightarrow Y$ such that $f(X_s) \subset Y_s$, and such a map is *stratified* if $f(X^s) \subset Y^s$. This leads to definitions of stratified homotopy, therefore stratified homotopy equivalence.

Immediate examples of stratified manifolds are manifolds with boundary and manifolds with corners. Many handles (e.g. $[0, 1] \times [0, 1]$) are manifolds with corners, and the result of a smooth handle attachment is a manifold with corners at $\varphi(\partial D^\lambda \times \partial D^\mu)$. Hence both are stratified manifolds.

A *stratified handle attachment* is a handle attachment where the handle, the manifold to which we attach the handle, and the attaching map are each stratified. The main distinctions between stratified handle attachment and handle attachment are:

1. the handle is necessarily stratified, though the stratification is not necessarily induced by the corners that occur in the standard formation of a handle as the Cartesian product of a pair of disks,
2. the manifold to which we attach the handle is necessarily stratified, and
3. the attaching map ensures that there is a coherent identification between the strata of the handle and the strata of the manifold (i.e. the stratification of the resulting attachment space is well-defined).

2.3 Handlebodies

Handlebodies are objects central to the arguments of Chapters 3 and 4. We use Gompf & Stipsicz [5] and Schleimer [12] as our main references for handlebodies. A

handlebody is formed by attaching some number of (n, λ) –handles to an $(n, 0)$ –handle. The name is evoked by the type of handlebody that we examine in this section: the $(3, 1)$ –handlebody.

Definition 2.3.1. A connected n –manifold M that has a handle decomposition consisting of exactly one 0–handle and g λ –handles is called an (n, λ) –*handlebody* of *genus* g .

Let V be an $(n, 1)$ –handlebody of genus g . A simple closed curve in ∂V is called *essential* if it is not homotopic to a point. A simple closed curve J in ∂V that is essential in ∂V and that bounds a 2–disc in V is called a *meridian*. The properly embedded disc in V that has boundary J is called a *meridinal disc*.

The special case of the oriented genus 1 $(m, 1)$ –handlebody is called a *solid torus*. More generally, any space that is homeomorphic to $S^1 \times D^{n-1}$ is called a *solid n –torus*. In our most common case of $n = 3$, we just say that $S^1 \times D^2$ is a *solid torus*. A simple closed curve J in the boundary of a solid torus that intersects a meridian at a single point is called a *longitude*. A longitude is essential in a solid torus and there are infinitely many isotopy classes of longitudes, but there is exactly one isotopy class of meridians.

We apply handlebodies to 3–manifold classification through Heegaard splittings.

Definition 2.3.2. Let U and V be 3–dimensional handlebodies of genus g and let $f : \partial U \rightarrow \partial V$ be an orientation preserving diffeomorphism. The adjunction $M = U \cup_f V$ is a *Heegaard splitting* of M , the shared boundary $H = \partial U = \partial V$ is the *Heegaard surface* of the splitting, and the shared genus of U and V is the *genus* of the splitting as well. A Heegaard splitting is also denoted by the pair (M, H) .

We use the notion of equivalence between splittings from [12]: A pair of splittings (M, H) and (M, H') are *equivalent* if there is a homeomorphism $h : M \rightarrow M$ such that h is isotopic to id_M and $h|_H$ is an orientation preserving homeomorphism $H \rightarrow H'$.

Example 2.3.3. The 3–sphere S^3 has two standard Heegaard splittings. The first is the genus 0 splitting, which is realized by considering S^3 as the set of unit vectors in \mathbb{R}^4 . Take the Heegaard surface to be the intersection of S^3 with the xyz –hyperplane in \mathbb{R}^4 . This is a copy of S^2 that separates S^3 into two connected components. This splitting is written (S^3, S^2)

The second is the genus 1 splitting, which is visualized using the realization of S^3 as the one–point compactification of \mathbb{R}^3 . Take solid tori U and V and identify

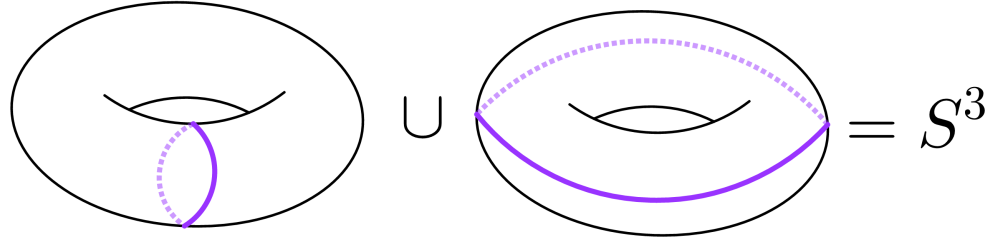


Figure 2.1: **Genus 1 Heegaard splitting of S^3** . The purple curve is essential in each solid torus pictured. In the left torus it is a meridian, on the right a longitude.

∂U with ∂V by the homeomorphism that swaps a meridian with a longitude. The adjunction is S^3 , and this splitting is written (S^3, T^2) . Figure 2.1 displays the tori of the splitting. This description of S^3 is also obtained by examining the boundary of a 4-dimensional 2-handle $\partial(D^2 \times D^2)$.

Definition 2.3.4. Let $(M, H) = U \cup_f V$ be a Heegaard splitting of M . The connected sum $(M, H) \# (S^3, T^2)$ is called an *elementary stabilization* of M , and itself is a splitting $(M, H \# T^2)$. A Heegaard splitting (M, H) is called a *stabilization* of another splitting (M, H') if it obtained from (M, H') via a finite number of elementary stabilizations.

Consider the meridians of the solid tori in the standard genus 1 splitting of S^3 . They each bound a disc in their respective handlebody, and they intersect in exactly one point. We would expect to be able to find such curves in any 3-manifold obtained as a stabilization.

Definition 2.3.5. Let $(M, H) = U \cup_f V$ be a Heegaard splitting of genus g and let α, β a pair of simple, closed, essential curves in H . Let α be a meridian of U and β be a meridian of V with associated meridinal discs D_α, D_β . If α and β intersect exactly once, then the pair (α, β) is a *meridinal pair* or *destabilizing pair* of the splitting.

To see why (α, β) would be called a destabilizing pair, remove a tubular neighbourhood of D_α from U and add it to V as a 2-handle along a tubular neighbourhood of α in H . In fact, the altered spaces U' and V' are handlebodies of genus $g - 1$ with $H' = \partial U' = \partial V'$, and (M, H) is a stabilization $(M, H') \# (S^3, T^2)$. We say that (M, H') is a *destabilization* of (M, H) over (α, β) . Note that when we consider β to be the belt sphere of a 1-handle and α to be the attaching sphere of a 2-handle, a destabilization is also a handle cancellation.

Chapter 3

Construction for smooth manifolds

We prove that every smooth, closed, orientable 3-manifold is the boundary of some 4-manifold. We do so by explicitly constructing such a 4-manifold from a given 3-manifold. This construction is mirrored in Chapter 4 where we prove the same for a given closed, orientable 3-manifold triangulation and provide an algorithm.

Let M be a smooth, closed, orientable 3-manifold and take $W = M \times [0, 1]$. Then W is a 4-manifold with boundary

$$\partial W = (M \times \{0\}) \cup (M \times \{1\}) = M_0 \cup M_1.$$

We construct a manifold with only one boundary component from W by attaching 4-dimensional 2-, 3-, and 4-handles to W over the part of its boundary away from M_0 . We start by attaching 2-handles to W over M_1 to produce a 4-manifold W' with boundary $M_0 \sqcup M'_1$, where $M'_1 = \partial W' \setminus M_0$ and is described via surgery on M_1 . We then attach 3-handles to W' over M'_1 to produce a 4-manifold W'' with boundary $M_0 \sqcup M''_1$. As before, $M''_1 = \partial W'' \setminus M_1$ and M''_1 is described via surgery on M'_1 . At this point in the construction, M''_1 is the disjoint union of a finite number of copies of S^3 . We attach 4-handles to W'' over M''_1 to produce a 4-manifold whose boundary is exactly M_0 .

Instructions for handle attachment come from defining a projection $f : M_1 \rightarrow \mathbb{R}^2$ that induces a stratification of $M_1 \subset \partial W$.

We call a closed 3-dimensional stratum of M_1 a *block*, and we impose conditions on f to ensure that every block can be classified up to *stratified homeomorphism*. We say that X, Y are *stratified homeomorphic* if X, Y are stratified spaces and there exists a homeomorphism $f : X \rightarrow Y$ such that f and f^{-1} are each stratified maps.

The blocks of M_1 are described below:

Face block: An attachment neighbourhood for a stratified 2–handle. Each face block is stratified-homeomorphic to $S^1 \times G_n$, the product of the circle with an n -gon for some n .

Edge block: A partial attachment neighbourhood for a stratified 3–handle. Each edge block is stratified-homeomorphic to one of $D^2 \times [0, 1]$, $A \times [0, 1]$, or $P \times [0, 1]$, where A is the annulus $S^1 \times [0, 1]$ and P is a pair-of-pants surface. Attachment of stratified (4,2)–handles over our face blocks “fill in” the annular boundary components of edge blocks, forming full attachment neighbourhoods for stratified 3–handles.

Vertex block: A partial attachment neighbourhood for a stratified 4–handle. Each vertex block is homeomorphic to a (3,1)-handlebody of genus at most 3. When stratified (4,2)– and (4,3)–handles are attached to W , the genus of these handlebodies are reduced until the remaining boundary of W consists of M_0 union a collection of stratified 3–spheres. The 3–spheres are then coned away.

The remainder of this chapter is spent ensuring that such a stratification can be achieved for any smooth, orientable, closed 3–manifold, detailing how the stratification is induced, proving that the attachment of stratified (4,2)– and (4,3)–handles has the previously stated effects, and discussing the resulting 4–manifold.

3.1 Projections from 3–manifolds to \mathbb{R}^2

Our stratification of M is induced by a decomposition of the plane, itself induced by the singular values of a smooth map $M \rightarrow \mathbb{R}^2$. To prove that a stratification suitable for our construction exists for any smooth orientable 3–manifold, we show first that an inducing decomposition of \mathbb{R}^2 exists. To prove that such a decomposition of \mathbb{R}^2 exists, we present the properties of $f : M \rightarrow \mathbb{R}^2$ required to induce the decomposition, and argue why a map possessing such properties exists for any smooth, orientable 3–manifold.

Let $f : M \rightarrow \mathbb{R}^2$ be a smooth map, let df be the differential of f , and let $S_r(f)$ be the set of points in M such that df has rank r . Then we require that the following be true of f :

1. $S_0(f)$ is empty.
2. $S_1(f)$ consists of smooth non-intersecting curves. We call these the *fold curves* of f .
3. The set of points where $f|_{S_1(f)}$ has zero differential is empty.
4. If $p \in S_1(f)$ then there exist coordinates (u, z_1, z_2) centred at p and (x, y) centred at $f(p)$ such that f takes the form of either
 - (a) $(x, y) = (u, \pm(z_1^2 + z_2^2))$, or
 - (b) $(x, y) = (u, \pm(z_1^2 - z_2^2))$
 in a neighbourhood of p . If f takes the form of 4a then we further classify p as a *definite fold*, and if f takes the form of 4b then p is an *indefinite fold*.
5. Let $\gamma_i, \gamma_j, \gamma_k \in S_1(f)$ be fold curves. Then each of $f(\gamma_i)$, $f(\gamma_j)$, $f(\gamma_k)$ are submanifolds of \mathbb{R}^2 such that
 - (a) $f(\gamma_i)$ and $f(\gamma_j)$ intersect transversely,
 - (b) $f(\gamma_i) \cap f(\gamma_j) \cap f(\gamma_k)$ is empty (i.e. there are no triple-intersections), and
 - (c) self-intersections of $f(\gamma_i)$ are transverse
6. The set of singular values of f in the plane is connected
7. The image of M through f is bounded in the plane.

We call these the *stratification conditions* on f , and we call a map satisfying the stratification conditions a *stratifying map*. The existence of smooth maps satisfying conditions 1–4 is discussed in [7], and 5–7 are straightforward. A smooth map satisfying conditions 1–4 can be smoothly perturbed inside of a tubular neighbourhood of $S_1(f)$ to satisfy conditions 5 & 6. Finally, condition 7 is always satisfied because the image of a compact set through a continuous map is compact.

3.2 Stratifying \mathbb{R}^2

Let $f : M \rightarrow \mathbb{R}^2$ be a stratifying map and let $X_f = f(S(f))$, the set of singular values of f . X_f is a connected collection of arcs in the plane that intersect only transversely.

We fit closed neighbourhoods (*sleeves*) around the singular values of f and classify these sleeves by the maximum codimension (with respect to \mathbb{R}^2) of singular values they contain. Because X_f consists of codimension 1 and codimension 2 singular values (arcs and arc-crossings respectively), we stratify \mathbb{R}^2 into face regions that contain no singular values, edge regions that contain only codimension 1 singular values, and vertex regions, each of which contain exactly 1 codimension 2 singular value. Figures 3.1-3.3 are used to illustrate the stratification resulting from sleeve-fitting.

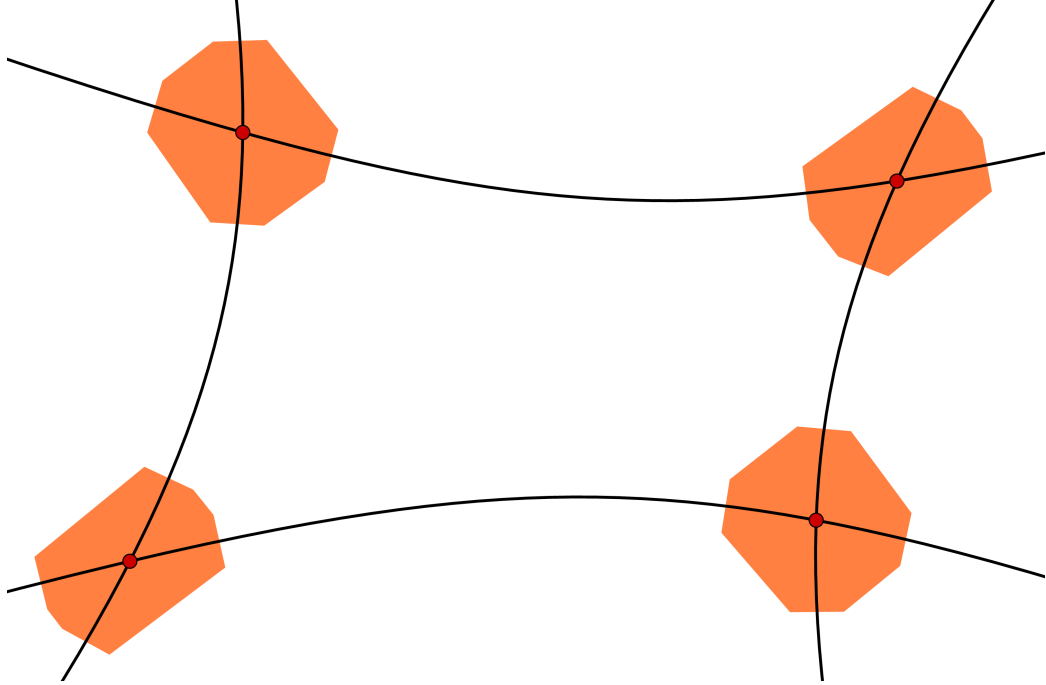


Figure 3.1: **Forming vertex regions.** Octagonal sleeves are fit around codimension 2 singular values to form vertex regions. Codimension 1 singular values are illustrated in black and their crossings, codimension 2 singular values, are indicated in red. Note that the edges of the octagonal sleeves alternate between containing exactly one singular value, its intersection with a black arc, or consisting entirely of regular values. New vertex regions are shaded orange.

We begin by fitting octagonal sleeves around codimension 2 singular values as in Figure 3.1. If x is a codimension 2 singular value then x is the result of an arc crossing, and a small neighbourhood around an arc crossing is divided into four regions of regular values. The octagon around x is fit so its edges alternate between being fully contained in a region of regular values and orthogonally intersecting one of the arcs of singular values that creates x . See Figure 3.1 for an example fitting.

The interiors of the octagons along with the octagonal boundaries form the vertex

regions of the stratification of \mathbb{R}^2 . The octagons are chosen to be small enough that no two vertex regions overlap and such that the octagonal edges that intersect arcs of codimension 1 singular values are all the same length.

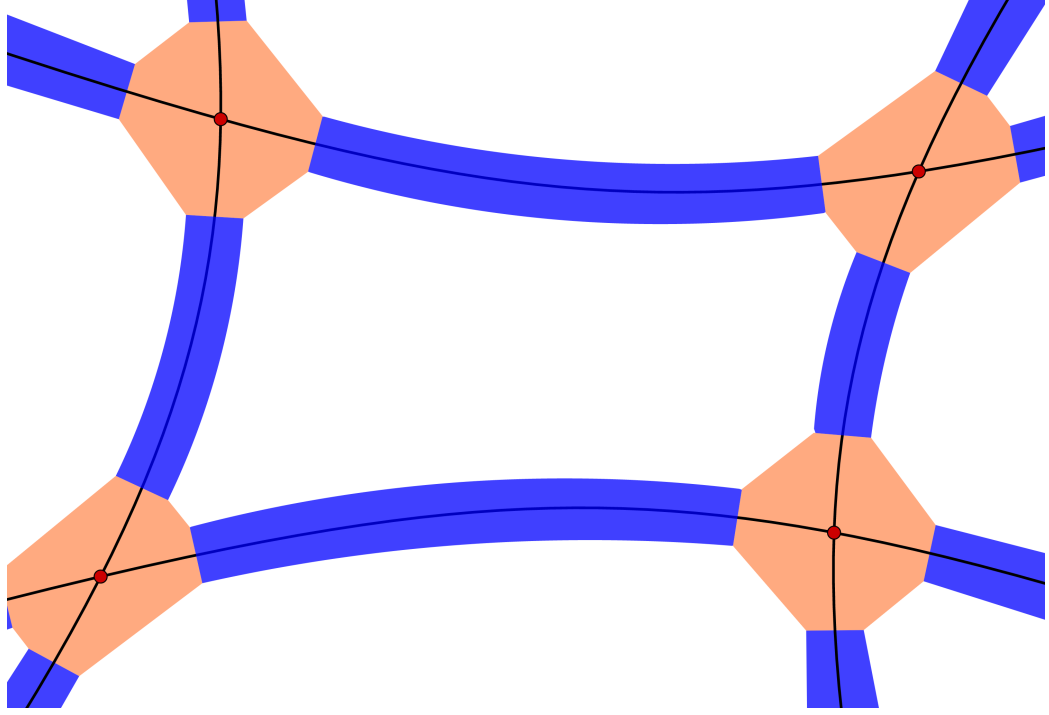


Figure 3.2: **Forming edge regions.** Vertex region corners are connected to fit sleeves around arcs of codimension 1 singular values to form edge regions. New edge regions are shaded blue.

Let γ be an arc of codimension 1 singular values with endpoints a pair of codimension 2 singular values. γ orthogonally intersects one edge from each of the octagonal vertex regions fit around its endpoints, and we use these edges to form the edge region associated to γ by connecting the endpoints of these edges to one another using a pair of arcs parallel to γ . See Figure 3.2 for an example fitting.

The closures of the interiors of the shapes formed by the arcs and octagon edges form the edge regions of the stratification of \mathbb{R}^2 . The octagonal edge endpoints are also vertices of the octagons, and the formation of edge regions uses every octagonal vertex as the endpoint of exactly one arc.

Removing from $f(M)$ all vertex and edge regions, we are left with a collection of connected regions in the plane, each of which consists entirely of regular values. The sixth stratification condition (that the set of singular values of f in the plane is connected) guarantees that each of these region is simply connected. This is because

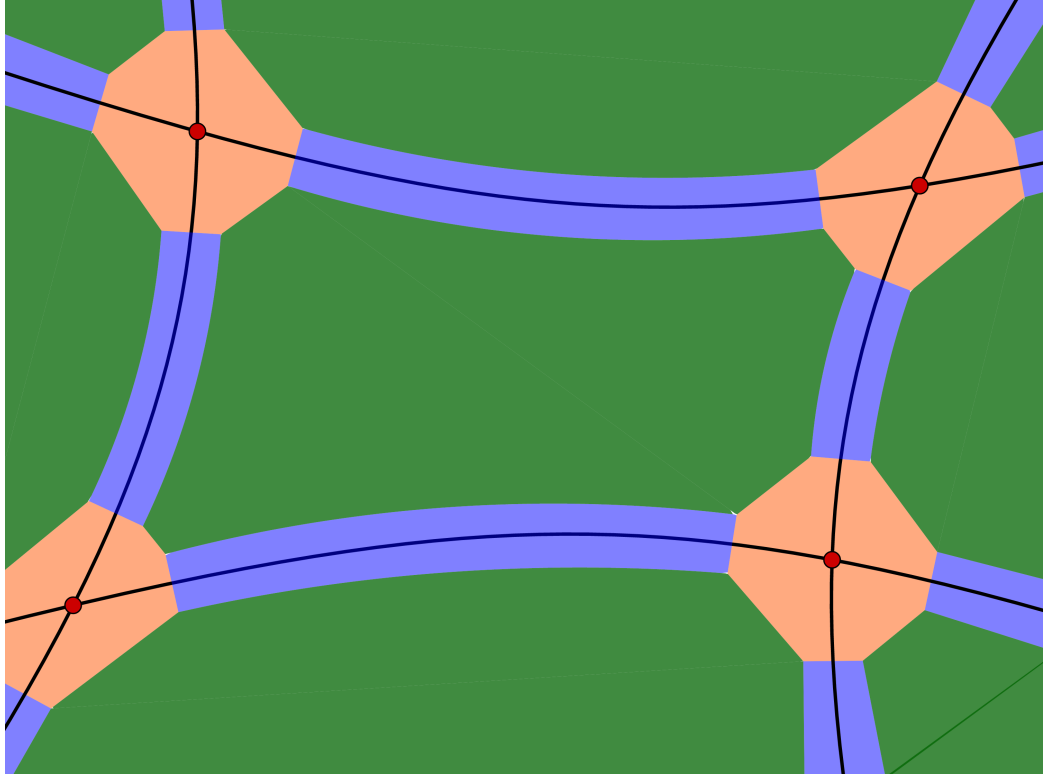


Figure 3.3: **Forming face regions.** All remaining regions contain no singular values, and we take these to be the face regions. New face regions are shaded green.

the boundary components of these regions are formed by the singular values of f in the plane, and different boundary components are necessarily disjoint. Note that a map satisfying the first five stratification conditions can be smoothly homotoped to satisfy the sixth condition, and this is argued by induction on the number of connected components of the set of singular values of f in the plane.

We take the closures of these to be the face regions of the stratification of \mathbb{R}^2 . The boundary of each face region is an alternating collection of arcs from edge regions and octagonal edges from vertex regions. See Figure 3.3 for an example fitting.

With all of the regions defined, we can describe precisely how f stratifies \mathbb{R}^2 . The stratification of \mathbb{R}^2 is a stratification into subsets $R_{(i,j)}$ where i, j are integers. Subset indexing is defined so that a subset $R_{(i,j)}$ is an i -dimensional submanifold of \mathbb{R}^2 , thus $R_{(i,j)} \not\subset R_{(k,l)}$ if $i \not\leq k$. The first collection of subsets used to filter \mathbb{R}^2 are the corners of the octagonal vertex sleeves. We assign to these subsets the indices $(0, i)$ for $i = 1 \dots N_0$, where N_0 is the number of corners. Corners are disjoint, so for any i, j with $i \neq j$, $R_{(0,i)}$ is not contained in $R_{(0,j)}$, hence $(0, i) \not\subset (0, j)$.

The boundary arcs connect the $(0, i)$ -level strata. Arcs are indexed by $(1, j)$ for $j = 1 \dots N_1$, where N_1 is the number of arcs. The boundary points of an arc are corners and are subsets of the filtration indexed by the $(0, i)$ indices, so $(0, i) \leq (1, j)$ if and only if $R_{(0, i)}$ is one of the boundary points of $R_{(1, j)}$. Arcs intersect only at their boundary points, so $(1, j) \not\leq (1, k)$ for any j, k .

The regions themselves are indexed by $(2, k)$ for $k = 1 \dots N_2$, where N_2 is the number of regions. These indices work similarly to the arc indices. The boundary of a region consists of corners and arcs, so $(n, i) \leq (2, k)$ if and only if $R_{(n, i)}$ is contained in the boundary of $R_{(2, k)}$.

With \mathbb{R}^2 stratified, we move onto a stratification of M . This stratification is induced by the preimages of the strata of \mathbb{R}^2 .

3.3 Stratifying M

Stratifying \mathbb{R}^2 via the singular values of f also induces a stratification of M by considering the fibers of f above the stratifying regions. The interiors of face regions have preimage through f a disjoint collection of face blocks, the interiors of edge regions have preimage of edge blocks, and of vertex regions, vertex blocks.

To understand the structure of face, edge, and vertex blocks we investigate the preimages of regular and singular values of f in the plane.

Definition 3.3.1. Because M is closed, f is proper. Thus, for any point q in $f(M)$, a fiber of f above q (i.e. a connected component of $f^{-1}(q)$) is either a closed 1-manifold (i.e. S^1) or contains a critical point of f .

We define a *singular fiber* to be a fiber that contains a critical point of f , and a *regular fiber* to be a fiber consisting entirely of regular points.

The subsets used to stratify M are the fibers of f that lie above the corners of the octagonal vertex regions, the edges of the vertex and edge regions, and the regions themselves. Because the corners of the vertex regions are regular values, their fibers are regular, hence a finite collection of disjointly embedded circles in M . We take these circles as the first collection of subsets that filter M , and assign to them the indices $(1, i)$ for $i = 1 \dots N_1$, where N_1 is the number of circles. These circles are disjoint, so $(1, i) \not\leq (1, j)$ for any i, j .

The arcs of the \mathbb{R}^2 stratification connect the vertices of the \mathbb{R}^2 stratification and either consist entirely of regular values or contain exactly one singular value. As

pictured in Figure 3.3, an arc contains exactly one singular value precisely when it is the boundary a vertex region and an edge region. When an arc contains exactly one singular value, exactly one fiber above that value is a singular fiber, with the rest regular fibers. A decomposing arc is diffeomorphic to the unit interval and f is a smooth submersion between smooth manifolds, so a fiber above a decomposing arc is a surface whose boundary circles are the fibers above the arc's endpoints. When the fiber is regular, the surface is diffeomorphic to an annulus $S^1 \times [0, 1]$. When the fiber is singular, the surface classification depends on the type of singularity. Theorem 3.3.2 and Figure 3.4 show that the fiber containing the singularity either has the structure of a figure-of-eight (when the singularity is part of an indefinite fold) or is a single point (when the singularity is part of a definite fold), hence the singular fiber above the arc is diffeomorphic to either a 2-disk or a pair-of-pants.

Theorem 3.3.2 refers to a *stable map*, and we'll denote the set of smooth stable maps $X \rightarrow Y$ by $Stab(X, Y)$. When X is a smooth, closed, orientable 3-manifold and Y is the plane, $Stab(X, Y)$ consists of all maps $X \rightarrow Y$ satisfying the first five stratification conditions. The last stratification condition is trivially satisfied because X is closed, hence the set of stratifying maps $X \rightarrow Y$ is the subset of $Stab(X, Y)$ consisting of maps f such that $f(S(f))$ is connected.

Theorem 3.3.2 (Adapted Theorem 3.15 in Saeki [11]). Let $f : M \rightarrow N$ be a proper C^∞ stable map of an orientable 3-manifold M into a surface N . Then, every singular fiber of f is equivalent to the disjoint union of:

1. one of the fibers in Figure 3.4, and
2. the disjoint union of a finite number of copies of S^1 .

Furthermore, no two fibers in the list are equivalent to each other even after taking the union with regular circle components.

The surface fibers above the decomposing arcs are the second collection of subsets that filter M , and they are assigned the indices $(2, j)$ for $j = 1 \dots N_2$, where N_2 is the number of surfaces. The boundary circles of the surfaces are each subsets of the filtration, indexed by the $(1, i)$ indices, so $(1, i) \leq (2, j)$ if and only if $M_{(1, i)}$ is one of the boundary components of $M_{(2, j)}$. These surfaces intersect one another only when they share a boundary circle, so $(2, j) \not\leq (2, k)$ for any j, k .

There are three types of region in the decomposition: face, edge, and vertex. Regardless of the type of region, they are indexed in our filtration similarly to the

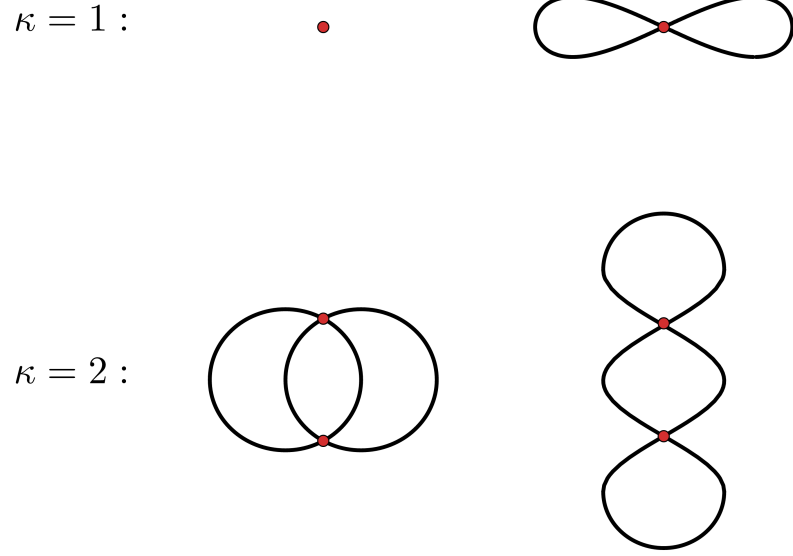


Figure 3.4: **Connected singular fibers.** List of connected singular fibers of proper C^∞ stable maps of orientable 3-manifolds into surfaces. κ is the codimension of the singularity in the surface. The singular fiber above a codimension 2 singular value may be disconnected, in which case the fiber is the disjoint union of a pair of singular fibers from $\kappa = 1$.

edges. A fiber above a region is a 3-manifold with corners formed by the $(1, i)$ - and $(2, j)$ -level strata, and fibers are disjoint away from their boundaries. We therefore index fibers above regions with the indices $(3, k)$ for $k = 1 \dots N_3$ where N_3 is the total number of fibers above regions, put $(n, i) \leq (3, k)$ if and only if $M_{(n, i)}$ is contained in the boundary of $M_{(3, k)}$.

Recall that we call a closed 3-dimensional stratum of M a *block*. We now restate the desired block structure laid out at the beginning of this chapter and prove that the stratification conditions impose this structure on the blocks of M .

Theorem 3.3.3. Let M be a smooth, closed, orientable 3-manifold, let $f : M \rightarrow \mathbb{R}^2$ be a stratifying map, suppose \mathbb{R}^2 has been decomposed as in Section 3.2 and M has been stratified as in this section. Then each closed strata $M_{(3, k)}$ is classified as either a *face*, *edge*, or *vertex block* depending on whether it is a fiber above a face, edge, or vertex region respectively, and a block has one of the following structures:

Face block: Let B be a face block that fibers over the face region F . Then B is stratified-homeomorphic to $S^1 \times F$.

Edge block: Let B be an edge block that fibers over the edge region E . Let A be the annulus $S^1 \times [0, 1]$ and P the pair-of pants surface (i.e. D^2 minus a pair of disjoint open balls). If B is a regular fiber over E then B is stratified-homeomorphic to $S^1 \times E$, hence also stratified-homeomorphic to $A \times [0, 1]$. Otherwise, B is a singular fiber over E and contains part of definite or indefinite fold. In this case we call B a *definite* or *indefinite edge block*. A definite edge block is stratified-homeomorphic to $D^2 \times [0, 1]$ and an indefinite edge block is stratified-homeomorphic to $P \times [0, 1]$.

Vertex block: Let B be a vertex block that fibers over the vertex region V . If B is a regular fiber then it is homeomorphic to $S^1 \times V$, therefore homeomorphic to a (3,1)-handlebody of genus 1. Otherwise, we see from Figure 3.4 that the singular fiber above the codimension 2 singularity contained in V is either connected or disconnected. If the singular fiber is disconnected then there are a pair of disjoint vertex blocks that each contain one of the singular fibers, hence part of a definite or indefinite fold. We therefore classify these blocks as *definite* or *indefinite vertex blocks*. If the singular fiber is connected, then the block containing it is an *interactive vertex block*. A definite (resp. indefinite) vertex block extends and connects definite (resp. indefinite) edge blocks, and is homeomorphic to a (3,1)-handlebody of genus 0 (resp. 2). An interactive vertex block is homeomorphic to a (3,1)-handlebody of genus 3.

Remark 3.3.4. The structures of the blocks described in Theorem 3.3.3 are roughly disk bundles over a representative fiber for the given region or, equivalently, regular neighbourhoods of that fiber. For a block that is a regular fiber, the representative is a circle. For a definite or indefinite block, the representative is the singular fiber containing a definite or indefinite fold, and for an interactive block the representative fiber is the singular fiber above the codimension 2 singular value.

Proof of Theorem 3.3.3. We split the proof into three parts. The first part proves that if a block B is a regular fiber over the region R then B is stratified-homeomorphic to $S^1 \times R$. In the second part, we prove that definite and indefinite blocks are stratified-homeomorphic to $D^2 \times [0, 1]$ or $P \times [0, 1]$ respectively. In the final part we discuss interactive vertex blocks, and show that they are homeomorphic to (3,1)-handlebodies of genus 3. Figures illustrate the block structures.

Part 1: Let B be a block over the region R , and suppose B consists entirely of regular fibers over R . Then $(B, R, f|_B, S^1)$ has the structure of a circle bundle

over R . A fiber bundle over a contractible space is trivial, so B is homeomorphic to $S^1 \times R$. Furthermore, this homeomorphism is stratified by ensuring the strata of B are mapped to the strata of $S^1 \times R$, where the stratification of $S^1 \times R$ is defined by the manifold with corners structure induced by the product topology.

Part 2: Let B be a definite or indefinite block over the region R . R is a subset of the plane homeomorphic to D^2 with an arc $\gamma_s \subset X_f$ of singular values running from one of its edges to another. Let γ_t be a second simple arc that crosses γ_s transversely, and consider the cross-sectional surface obtained by $f^{-1}(\gamma_t)$. Figure 3.5 illustrates the possible surfaces containing the singular fiber over $x = \gamma_s \cap \gamma_t$.

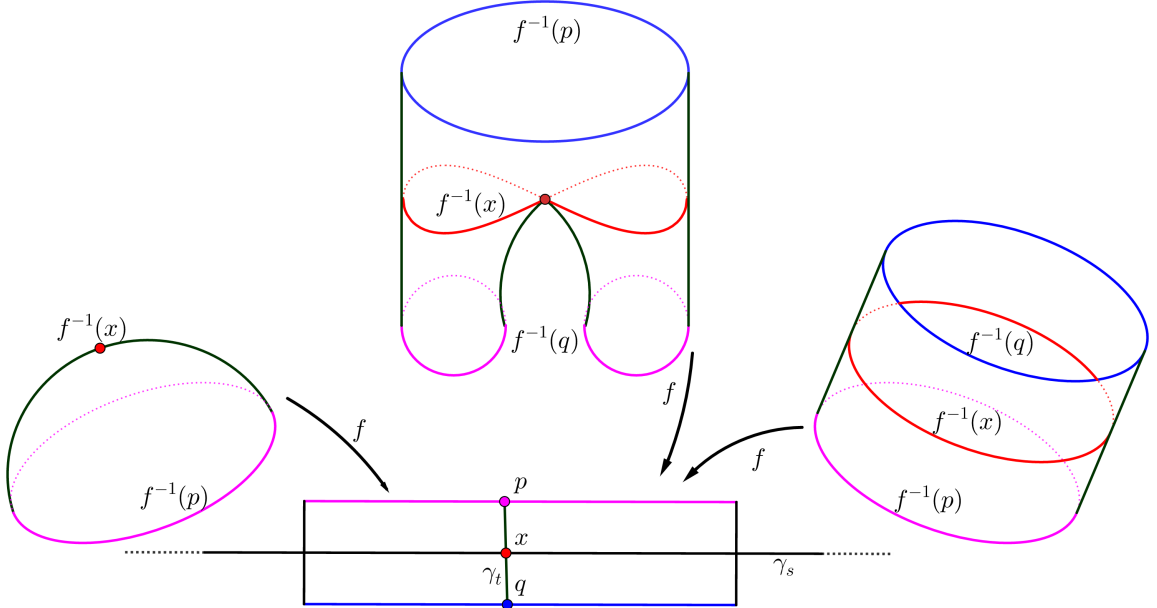


Figure 3.5: **Surfaces over codimension 1 singularities.** γ_s is an arc of singular values and γ_t is an arc with endpoints $\partial\gamma_t = \{p, q\}$ that intersects γ_s transversely at $x = \gamma_s \cap \gamma_t$. The three surfaces shown are the three possible cross-sectional surfaces that can project through f over γ_t .

This cross section is general, so we fit a tubular neighbourhood $\nu(\gamma_s)$ about γ_s in R to obtain a bundle structure for $f^{-1}(\nu(\gamma_s))$ whose fiber is one of the cross-sectional surfaces (a disk or a pair-of-pants) and whose base is the arc γ_s , i.e. an interval. The interval is contractible, so $f^{-1}(\nu(\gamma_s))$ is homeomorphic to $\Sigma \times [0, 1]$ for Σ a disk or a pair-of-pants surface. Away from $\nu(\gamma_s)$, R consists entirely of regular values so we obtain solid tori (cf. Part 1) that extend the $\Sigma \times [0, 1]$ structure as seen in Figure 3.6.

As with Part 1, the homeomorphism described is stratified by ensuring the strata of B are mapped to the strata of $\Sigma \times [0, 1]$, where the stratification of $\Sigma \times [0, 1]$ is

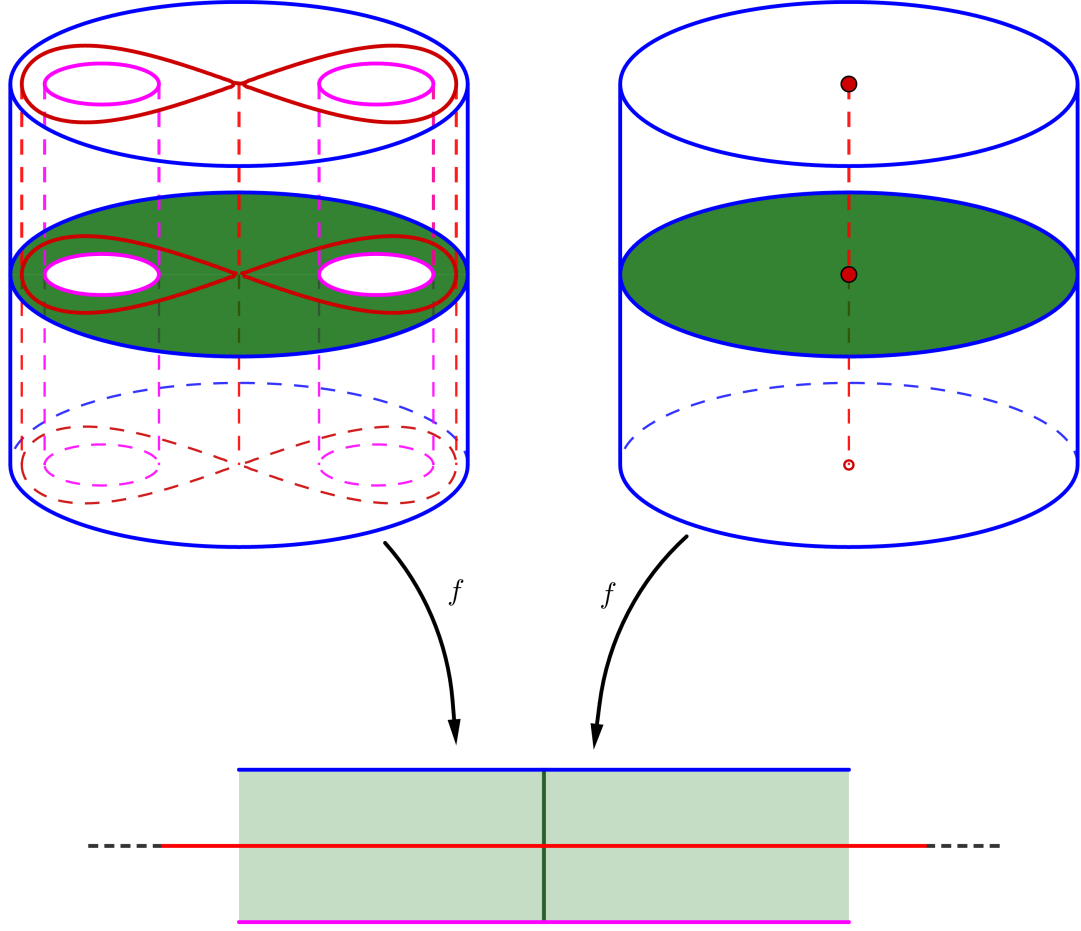


Figure 3.6: **Definite and indefinite blocks.** The blocks containing sections of definite and indefinite folds that project over codimension 1 singular values. These are found as singular fibers over edge and vertex regions.

defined by the manifold with corners structure induced by the product topology.

Part 3: Let B be an interactive block over the region R . Interactive blocks occur over octagonal vertex regions where the singular fiber above the region's codimension 2 singularity is connected, so we investigate these fibers. The codimension 2 singular value lies at the intersection of a pair of arcs of codimension 1 singular values. Call the arcs γ_1 and γ_2 , let $x = \gamma_1 \cap \gamma_2$, and denote the interactive singular fiber over x by $B_x = B \cap f^{-1}(x) = \{b \in B \mid f(b) = x\}$. Our method of investigation begins by examining the possible resolutions of B_x and combining those resolutions to form a genus 3 surface.

Figure 3.7 demonstrates resolutions of the singular points of B_x when B_x has the

first interactive singular fiber form presented in Figure 3.4. We first note that all of the displayed fibers have inherited an orientation from M . This forces fiber resolution to be unambiguous, and allows us to identify fibers when forming the surface shown in Figure 3.8.

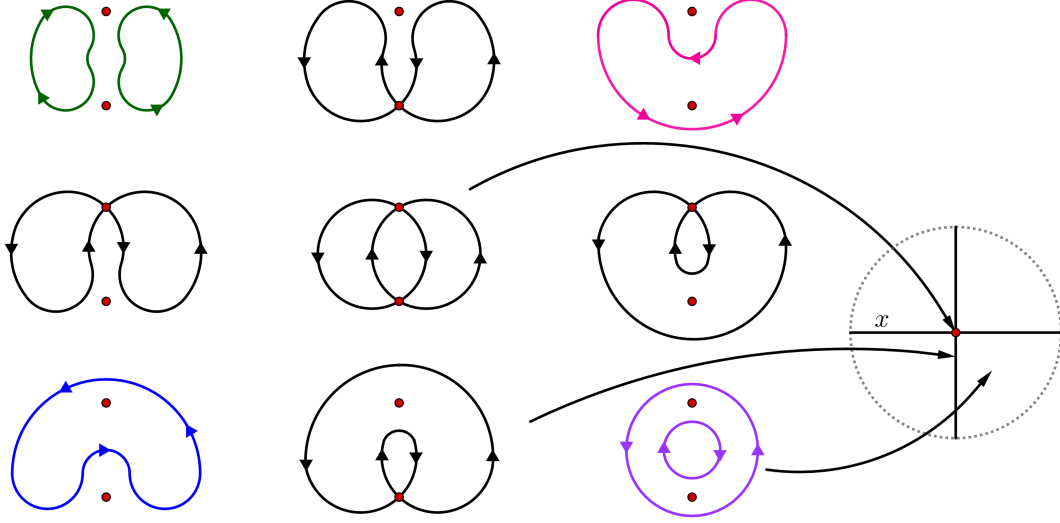


Figure 3.7: **Resolutions of the singular points in the first interactive fiber.** The singular fiber inside of B_x and its possible resolutions over nearby codimension 1 singular values and regular values. The fibers inherit orientation from M , and this illustration is presented without loss of generality. This figure is modeled after Figure 18 from [3].

We form the surface shown in Figure 3.8 by gluing together surfaces that project over simple arcs transversing the codimension 1 singular values. Gluing is performed over the boundary circles of these surfaces, and is prescribed by the resolutions in Figure 3.7. The transverse preimage containing the left column of fibers in Figure 3.7 is a pair of pants with two green ‘cuffs’ (top left) and a blue ‘waist’ (bottom left). The preimage containing the top row is a pair of pants with two green cuffs (top left) and a pink waist (top right). The first gluing that helps realize the surface in Figure 3.8 is of the ‘left’ transverse preimage surface with the ‘top’ transverse preimage surface over their shared green cuffs. The surfaces recovered as transversal preimages are then:

Left: a pair of pants with blue waist and green cuffs

Top: a pair of pants with pink waist and green cuffs

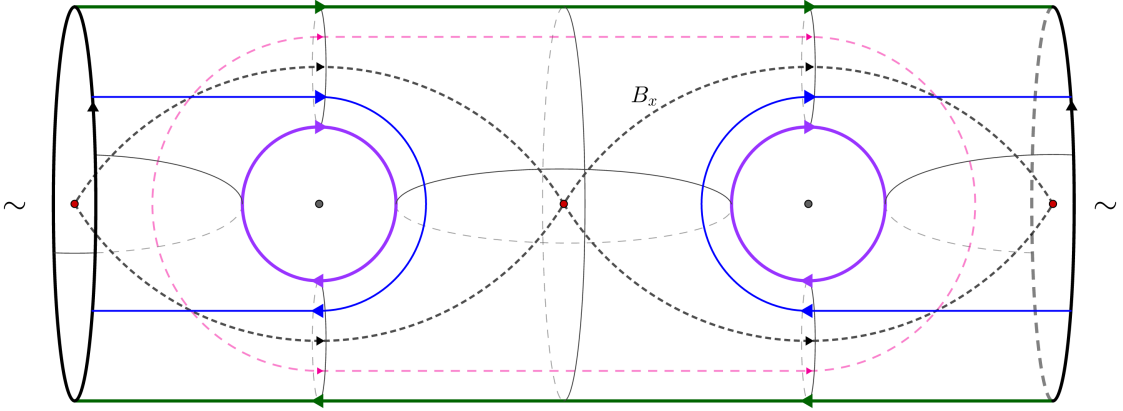


Figure 3.8: **Surface Σ near the first interactive fiber that projects over $\partial\bar{\nu}(x)$.** The surface and B_x are presented as embedded in S^3 , where $H(B_x)$ is the genus-3 (3,1)–handlebody on the ‘inside’ of Σ in S^3 .

Right: a pair of pants with pink waist and purple cuffs

Bottom: a pair of pants with blue waist and purple cuffs

The surface Σ in Figure 3.8 is the boundary of $H(B_x)$, a regular neighbourhood of B_x in M , i.e. a genus-3 (3,1)–handlebody inside of M . $H(B_x)$ projects through f over $\bar{\nu}(x)$, a closed tubular neighbourhood of x , and Σ projects over $\partial(\bar{\nu}(x))$.

Figure 3.8 presents Σ and B_x as objects embedded in S^3 , where Σ bounds genus-3 (3,1)–handlebodies on both sides. We take the ‘inside’ component of $S^3 \setminus \Sigma$ (i.e. the component containing B_x) to be $H(B_x)$.

Outside of $\bar{\nu}(x)$ we use the investigations from Parts 1 and 2 of this proof. The rest of R , $f^{-1}(R \setminus \bar{\nu}(x))$, has the structure of a Σ -bundle over the interval, and the bundle extends $H(B_x)$ to the boundary of R , preserving the structure as a genus-3 (3,1)–handlebody. We conclude that B is homeomorphic to a genus-3 (3,1)–handlebody.

An identical argument is made when B_x has the second interactive singular fiber form, using Figures 3.9 and 3.10 in place of Figures 3.7 and 3.8 respectively. In this case the surfaces recovered as transversal preimages are:

Left: a pair of pants with blue waist and green cuffs

Top: the disjoint union of a pair of pants with green waist and pink cuffs with an annulus with one green boundary circle and one pink boundary component

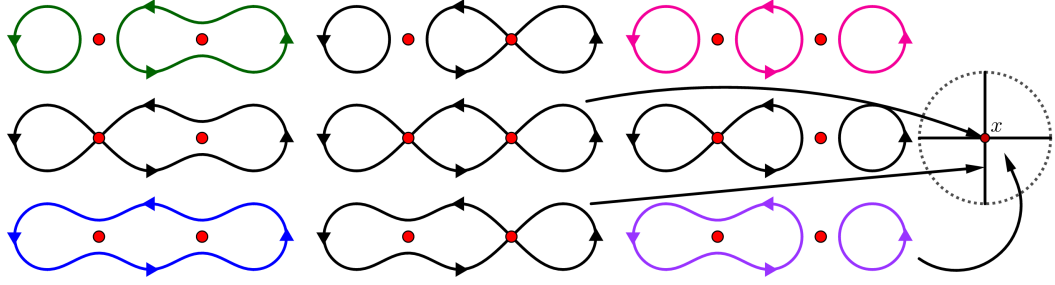


Figure 3.9: **Resolutions of the singular points in the second interactive fiber.** The singular fiber inside of B_x and its possible resolutions over nearby codimension 1 singular values and regular values. The fibers inherit orientation from M , and this illustration is presented without loss of generality. This figure is modeled after Figure 16 from [3].

Right: the disjoint union of a pair of pants with purple waist and pink cuffs with an annulus with one purple boundary circle and one pink boundary component

Bottom: a pair of pants with blue waist and purple cuffs

□

A smooth map f satisfying the stratification conditions of Section 3.1 induces a decomposition on \mathbb{R}^2 and a stratification of M . It is important to note here that the restrictions on f can induce a wide variety of possible stratifications of M , highlighting the variability of the resulting 4-manifold. We end this section with a lemma that guarantees the stratified 2-handle attachments of the next section can be made over our face blocks in any order, hence we can assume all attachments occur simultaneously.

Lemma 3.3.5. Let M be a 3-manifold with stratification induced as in Theorem 3.3.3. Then blocks of the same type (i.e. face, edge, vertex) are disjoint.

Proof. The fibers above a given region are disjoint, so the blocks above that region are disjoint. Regions of the same type are disjoint, hence blocks that are fibers above differing regions are also disjoint. □

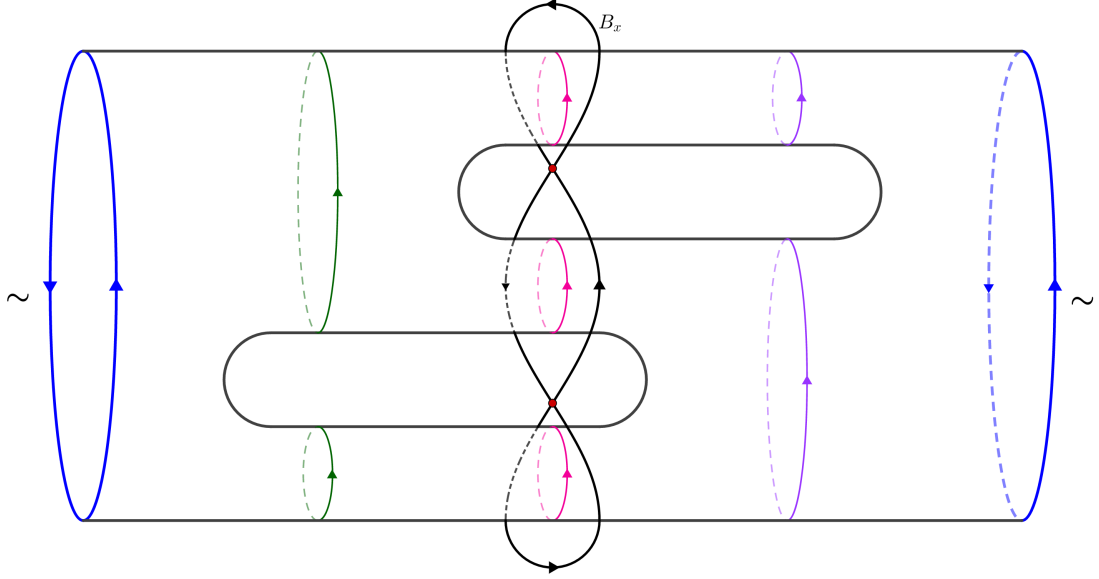


Figure 3.10: **Surface Σ near the second interactive fiber that projects over $\partial\bar{v}(x)$.** The surface and B_x are presented as embedded in S^3 , where $H(B_x)$ is the genus-3 (3,1)–handlebody on the ‘outside’ of Σ in S^3 .

3.4 Attach Handles

Stratifying M allows the definition of attachment neighbourhoods for stratified 2–, 3–, and 4–handles in $W = M \times [0, 1]$. A 4–dimensional 2–handle is attached over a closed solid torus embedded in the boundary of a 4–manifold, so attachment neighbourhoods for our stratified 2–handles are straightforward: they are the face blocks of M . We alter the boundary of W by attaching handles, so the attachment neighbourhoods for 3–handles (4–handles, resp.) must be found after 2–handles (3–handles, resp.) are attached. For a 3–handle, an attachment neighbourhood consists of the union of an edge block with some strata introduced by 2–handle attachment. For a 4–handles, an attachment neighbourhood consists of the union of an edge block with some strata introduced by 2– and 3–handle attachment. We investigate the consequences of handle attachment by comparing the boundary of the initial manifold with the boundary of the manifold resulting from handle attachment, and use a precisely defined handle structure to focus the investigation. Our first step is to precisely define the structure of the stratified 2–handles that we are attaching.

3.4.1 2–handles

Let B be a face block of M_1 . By Theorem 3.3.3, B is a closed solid torus that is stratified-homeomorphic to $S^1 \times G_n$, where G_n is an n -gon for some n . Consider an unknotted embedding of B in S^3 . The complement of the interior of B is another closed solid torus B' . The tori B and B' are depicted as cylinders with top and bottom identified in Figure 3.11.

We stratify B' as follows. First include the shared stratified boundary of B . Next, introduce meridional disks of B' that are bounded by the $(1, i)$ -indexed strata in B , i.e. the boundary curves in B corresponding to $S^1 \times c_m$ where c_m is a corner of G_n , $m = 1 \dots n$. Finally, add the homeomorphic 3-disks of B' whose boundaries consist of one longitudinal annulus of B along with the two meridional disks in B' that are bounded by the annulus's circular boundary components. The filtration of B' is created identically to that of the original face blocks, using inclusion as a partial ordering and indexing a stratum by its dimension as a submanifold of B' . Figure 3.11 illustrates a face block B and its complement inside of S^3 .

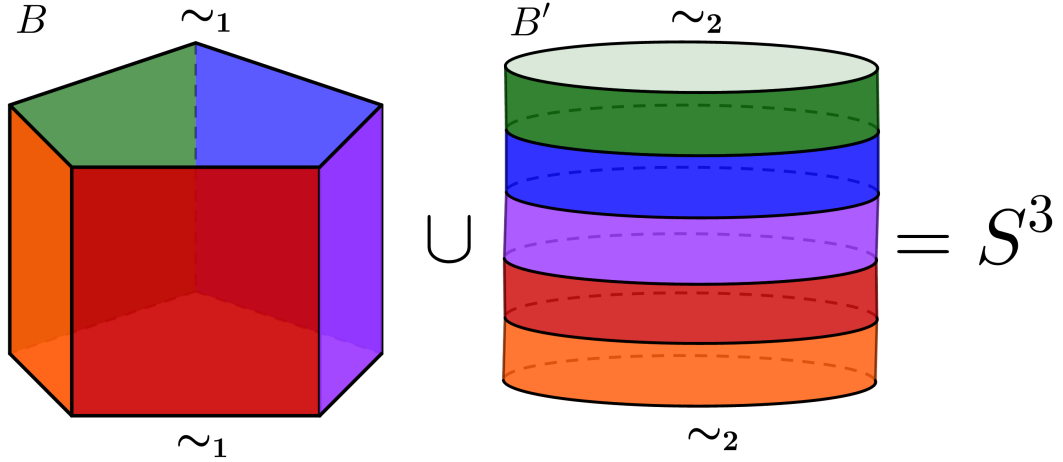


Figure 3.11: **A face block and its complement form S^3 .** A face block B is a stratified closed solid torus that is stratified-homeomorphic to $S^1 \times G_n$ for some n -gon G_n . The complement of its unknotted interior in S^3 is another stratified closed solid torus B' . B and B' are depicted as cylinders with top and bottom identified.

Taking S_B^3 to be the stratified S^3 formed as the union of B and B' , we craft a stratified 2–handle structure as $C(S_B^3)$, the cone of S_B^3 . We call $C(S_B^3)$ the *stratified 2–handle induced by B* . Attaching $C(S_B^3)$ to W over $B \subset M_1$ alters the boundary of W by replacing $B \subset M_1$ with B' . The full extent of this surgery can be detected by

examining the edge and vertex blocks of the stratification that are incident to B .

Theorem 3.4.1. Let M be a smooth, closed, stratified, orientable 3-manifold with stratification induced by a stratifying map f , let \mathfrak{B} be the set of face blocks of M_1 , and let $W = M \times [0, 1]$. Consider the 4-manifold W' constructed from W as

$$W' = W \cup \{C(S_B^3)\}_{B \in \mathfrak{B}} / \sim,$$

where \sim is defined by $b \sim \iota(b)$, ι the identity map $C(S_B^3) \supset B \xrightarrow{\iota} B \subset M_1$. Then $M'_1 = \partial W' \setminus M_0$ is a stratified 3-manifold with a decomposition into *primed edge blocks* and *primed vertex blocks* such that the decomposition is well-defined and the primed blocks have the following structure:

Primed edge block: A primed edge block E' is identical to an edge block E from Theorem 3.3.3 with (3,2)-handles (i.e. cylinders: $D^2 \times [0, 1]$) attached over all annular boundary strata of E (i.e. each closed strata A of E such that $A = E \cap B$ for some face block $B \in \mathfrak{B}$). Thus E' is a stratified 3-manifold homeomorphic to $S^2 \times [0, 1]$

Primed vertex block: A primed vertex block V' is identical to a vertex block V from Theorem 3.3.3 with (3,2)-handles attached over each annular boundary stratum A of V such that $A = V \cap B$ for some face block $B \in \mathfrak{B}$. Furthermore, we show that V' is a stratified (3,2)-handlebody.

Proof. We split the proof of this theorem into three parts. In the first two parts, we prove that we can find the prescribed primed edge and vertex block structures in M'_1 . In the third part, we show that these structures exhaust M'_1 .

Part 1: Edge blocks occur in three possible forms: regular edge blocks as $A \times [0, 1]$, definite edge blocks as $D^2 \times [0, 1]$, and indefinite edge blocks as $P \times [0, 1]$. Figure 3.12 displays the possible edge block forms and indicates the boundary strata of an edge block that are shared by face blocks.

Figure 3.13 illustrates how 2-handle attachment affects edge blocks. The effect on ∂W near E of attaching the (4,2)-handle $C(S_B^3)$ over B is equivalent to attaching a (3,2)-handle from the stratification of B' to E over the annular boundary stratum $E \cap B$. Attachment of all (4,2)-handles to W applies this (3,2)-handle attachment to all annular strata of E , and attaching these (3,2)-handles to all annular strata of E results in a 3-manifold homeomorphic to $S^2 \times [0, 1]$.

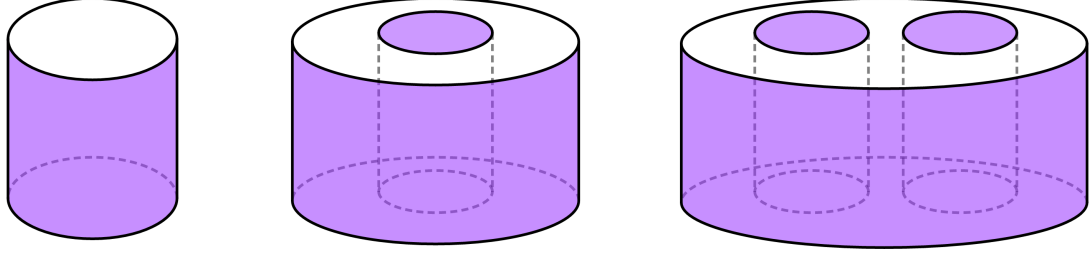


Figure 3.12: **Edge blocks.** The possible edge blocks of M_1 . Annular boundary strata that are incident with face blocks of M_1 are indicated in purple. For each block, attaching $(3,2)$ -handles over the indicated annuli results in a stratified 3-manifold homeomorphic to $S^2 \times [0, 1]$.

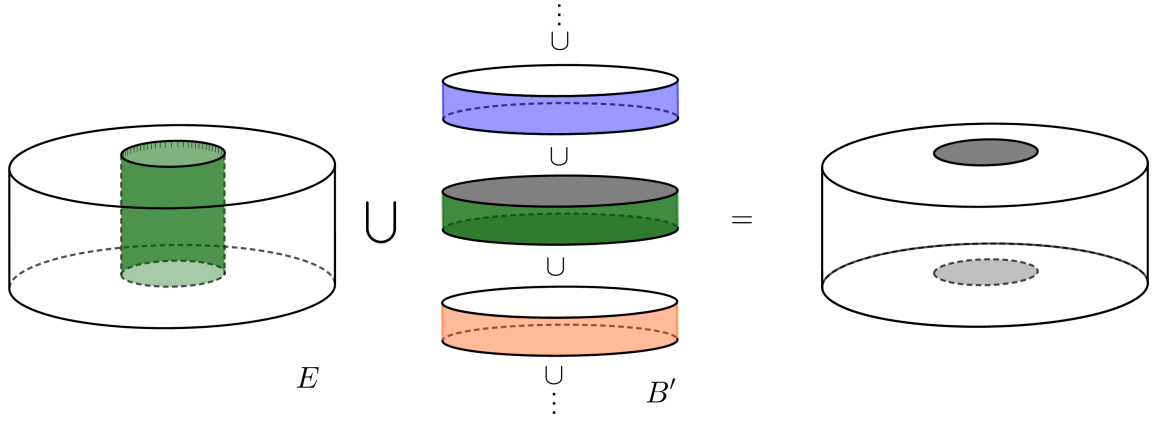


Figure 3.13: **The effect of stratified $(4,2)$ -handle attachment on an example edge block.** An edge block E , a face block complement B' , and the result of attaching $C(S_B^3)$ to W over B on E . The boundary stratum shared by E and B in M_1 is indicated in green, as is the corresponding boundary stratum of B' in S_B^3 .

Part 2: Let V be a vertex block. All vertex blocks are stratified $(3,1)$ -handlebodies of some genus, and V and V' are related via $(3,2)$ -handle attachments to V induced by $(4,2)$ -handle attachments. The attaching regions are disjoint, so the resulting manifold is independent of the order in which we attach handles.

Let g be the genus of V . Proving that V' is a $(3,2)$ -handlebody when $g = 0$ is trivial, because V is then a 3-ball. This means V' is a 3-ball with a collection of $(3,2)$ -handles attached to it, i.e. a $(3,2)$ -handlebody. The case of $g > 0$ is nontrivial.

Suppose V is a $(3,1)$ -handlebody of genus $g > 0$. To prove that V' is a $(3,2)$ -handlebody, we show that each $(3,2)$ -handle attachment either cancels a $(3,1)$ -handle of V or adds a new S^2 boundary component away from the $(3,1)$ -handles of V . When $g > 0$, V is a regular neighbourhood of either a circle or one of the nontrivial singular

fibers in Figure 3.4. Each case provides a (3,1)–handlebody structure for V . Because we are interested in handle cancellation, the salient point is the identification of (3,1)–handle belt spheres. When V is a solid torus, i.e. a regular vertex block, we set any meridinal circle of V as a belt sphere for the (3,1)–handle. Otherwise, give the fiber the graph structure implied by Figure 3.4. Then V has a (3,1)–handlebody structure with one or two (3,0)–handles, depending on the number of singular points in the fiber (i.e. vertices in the graph structure), and a (3,1)–handle for each edge.

With a (3,1)–handlebody structure in place, let α_i be the belt spheres of each (3,1)–handle. This implies that the α_i are pairwise non-parallel. Let β_i be the attaching spheres of the (3,2)–handles that we attach to V in the construction of V' . For each i, j , $|\alpha_i \cap \beta_j| = 0$ or 1 by construction. Moreover, for every i , $\alpha_i \cap \{\beta_j\}_j > 0$ and $\beta_i \cap \{\alpha_j\}_j > 0$. In words, every (3,1)–handle belt sphere transversely intersects at least one of the (3,2)–handle attaching spheres, every (3,2)–handle attaching sphere intersects at least one of the (3,1)–handle belt spheres, and all intersection numbers are at most 1. Thus every (3,2)–handle attached to V either cancels out an existing (3,1)–handle or adds a new 2–sphere boundary component. Because $\partial V'$ is a disjoint collection of 2–spheres we conclude that every (3,1)–handle of V has been cancelled by a (3,2)–handle, thus V' is a (3,2)–handlebody. We present an example of how these handle attachment sites are arranged in Figure 3.14.

Part 3: To show that primed edge and vertex blocks exhaust M'_1 , we show that the entirety of B' has been apportioned among the primed blocks for each B' . The $(3, k)$ strata of B' are each cylinders whose annular boundary strata corresponds directly to a longitudinal boundary annulus of B . Face regions do not intersect even on their boundary, so all of the annular boundary strata of B , hence B' , are shared only by edge and vertex blocks. Thus each cylinder of B' has been assigned as a (3,2)–handle and attached to a primed edge or vertex block. Because (4,2)–handle attachment altered M_1 to M'_1 only by replacing each face block B with its complementary B' , the primed blocks must exhaust M'_1 . \square

3.4.2 3–handles

Decomposing M'_1 into primed edge and vertex blocks provides us with stratified 3–handle attachment neighbourhoods. A 4–dimensional 3–handle is attached over an $S^2 \times [0, 1]$ embedded in the boundary of a 4–manifold, so attachment neighbourhoods for our stratified 3–handles are the primed edge blocks of M'_1 . We begin 3–handle

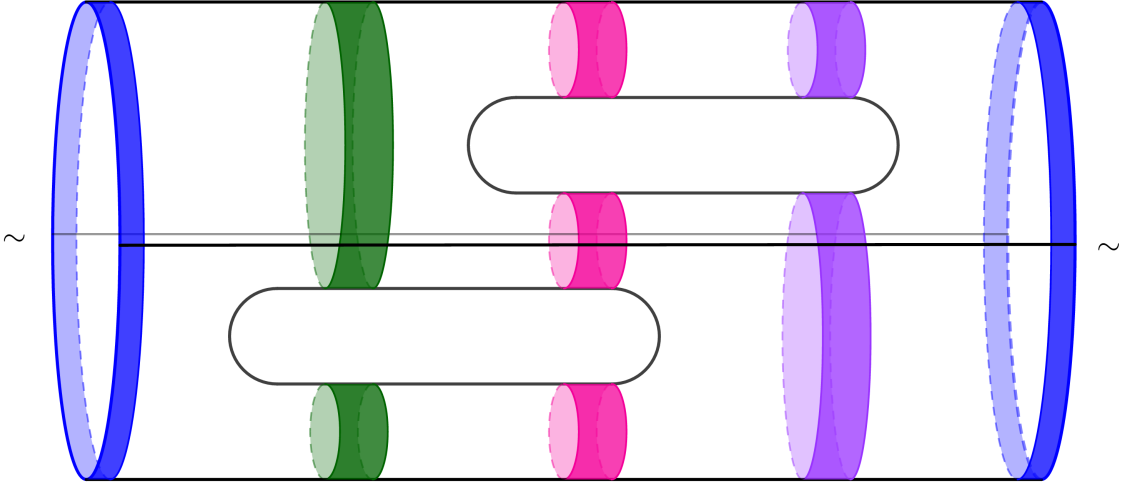


Figure 3.14: **Vertex block with (3,2)–handle attachment sites indicated.** We display an example vertex block of M_1 . Recall that this is the second type of interactive vertex block and, as in Figure 3.10, the surface is presented as embedded in S^3 and the block is the stratified (3,1)–handlebody on the ‘outside’ of the surface in S^3 . Annular boundary strata that are incident with face blocks of M_1 are indicated in color and correspond to the shared vertex-face region boundary edge. The 1–handle belt spheres are also indicated as black horizontal arcs across the surface. Attaching (3,2)–handles over the indicated annuli as prescribed results in a (3,2)–handlebody.

attachment by precisely defining the structure of a stratified 3–handle so that it may be attached over a primed edge block.

Let E' be a primed edge block of M'_1 . By Theorem 3.4.1, E' is homeomorphic to $S^2 \times [0, 1]$. In particular, $\partial E'$ is a disjoint pair of stratified 2–spheres. We form a 4–disk containing E' in its boundary by a double coning method on E' : we first cone the spherical boundary components of E' to form a pair of 3–disks, glue these 3–disks to E' to form a 3–sphere, then cone the 3–sphere to obtain a 4–disk.

For each stratified boundary sphere $S_i^2 \in \partial E'$ we form the stratified 3–disk $C(S_i^2)$ and glue $C(S_i^2)$ to E' over S_i^2 . The result is a stratified 3–sphere, and we further cone that 3–sphere to form a stratified 4–disk. We denote the 4–disk by $C^2(E')$ and call the resulting stratified 3–handle structure the *stratified 3–handle induced by E'* . Attaching $C^2(E')$ to W' over $E' \subset M'_1$ alters the boundary of W' by replacing E' with the 3–disks $C(S_i^2)$ glued over the corresponding stratified boundary spheres in M'_1 . The full extent of this surgery can be detected by examining the primed vertex blocks of M'_1 in Corollary 3.4.2.

Corollary 3.4.2. Let W' be the 4–manifold resulting from the construction described

in Theorem 3.4.1 and let \mathfrak{E}' be the set of primed edge blocks of $M'_1 \subset \partial W'$. Consider the 4-manifold W'' constructed from W' as

$$W'' = W' \cup \{C^2(E')\}_{E' \in \mathfrak{E}'} / \sim,$$

where \sim is defined by $e \sim \iota(e)$, ι the identity map $C^2(E') \supset E' \xrightarrow{\iota} E' \subset M'_1$. Then $M''_1 = \partial W'' \setminus M_0$ is a stratified 3-manifold with a decomposition into *double primed vertex blocks* V'' such that the decomposition is well-defined and each V'' is homeomorphic to S^3 .

Proof. We need only prove that each connected component of M''_1 is homeomorphic to S^3 . Let V' be a primed vertex block. We know that V' is a (3,2)-handlebody and $\partial V'$ is a disjoint collection of 2-spheres. Thus the attachment of (3,3)-handles to V' over each 2-sphere boundary component results in a 3-sphere, proving the theorem. \square

After attaching 3-handles over primed edge blocks, W'' is a 4-manifold with boundary consisting of M_0 and a collection of stratified 3-spheres. We attach stratified 4-handles over these 3-spheres, so we begin by precisely defining the structure of these handles.

3.4.3 4-handles

Let V'' be a double primed vertex block of M''_1 . By Corollary 3.4.2, V'' is homeomorphic to S^3 . We form a 4-disk whose boundary is V'' by taking the cone of V'' . We denote this 4-disk by $C(V'')$ and call the resulting 4-handle structure the *stratified 4-handle induced by V''* . Attaching $C(V'')$ to W'' over V'' alters the boundary of V'' by replacing it with \emptyset .

Corollary 3.4.3. Let W'' be the 4-manifold resulting from the construction described in Corollary 3.4.2 and let \mathfrak{V}'' be the set of double primed vertex blocks of $M''_1 \subset \partial W''$. Consider the 4-manifold W''' constructed from W'' as

$$W''' = W'' \cup \{C(V'')\}_{V'' \in \mathfrak{V}''} / \sim,$$

where \sim is defined by $v \sim \iota(v)$, ι the identity map $C(V'') \supset V'' \xrightarrow{\iota} V'' \subset M''_1$. Then $M'''_1 = \partial W''' \setminus M_0 = \emptyset$, hence W''' is a 4-manifold whose boundary is exactly M .

Chapter 4

Algorithm for triangulated manifolds

Algorithmic construction of a triangulated 4-manifold with a prescribed closed, orientable 3-manifold boundary broadly follows the steps we used in the construction of a 4-manifold with prescribed smooth, orientable 3-manifold boundary. Let N be a closed, orientable 3-manifold triangulation. Then the steps of construction are:

1. Define a projection $f : N \rightarrow \mathbb{R}^2$.
2. Induce a subdivision of N from f . The result is a 3-dimensional cell complex M that is equivalent to N . $M \times [0, 1]$ is a 4-dimensional cell complex with boundary components $M_0 = M \times \{0\}$ and $M_1 = M \times \{1\}$. Let W be the triangulation obtained by inductively triangulating each cell of M .
3. Attach 4-dimensional 2-handles to W over its M_1 boundary as prescribed by the subdivision of M from f . Call the result W' and let $M'_1 = \partial W' \setminus M_0$.
4. Form W'' by attaching 4-dimensional 3-handles to W' over M'_1 as prescribed by the subdivision induced by f and the surgery induced by 2-handle attachment.
5. The boundary of W'' consists of M_0 and a collection of copies of S^3 . Attaching a 4-handle to each S^3 boundary component results in a triangulated 4-manifold whose boundary is exactly M_0 .

This construction has input a closed, orientable 3-manifold triangulation N and output a 4-manifold triangulation W''' whose sole boundary component is a triangulated 3-manifold that is equivalent to N . In this case, we find that $\partial W'''$ is a

subdivision of N , and this subdivision is the subdivision induced by the projection f in Step 1.

It is necessary that the input 3-manifold triangulation is *edge-distinct*, i.e. if u, v are vertices of N then $\{u, v\}$ is the boundary of at most one edge. If this condition is not satisfied by a given N , then it is satisfied by the barycentric subdivision of N . We assume that N is edge-distinct for the remainder of the chapter.

Throughout this chapter N refers to the input closed, orientable 3-manifold triangulation, f refers to the subdividing map defined in Section 4.1, M is the subdivision of N induced by f , W is the 4-manifold triangulation obtained from $M \times [0, 1]$, W' is the result of attaching 2-handles to W , and W'' is the result of attaching 3-handles to W' .

4.1 Define projection

In this algorithm, we use a projection of $f : N \rightarrow \mathbb{R}^2$ in the same way that we used a stratifying map in Chapter 3: preimages of sleeves around important features of the projection in the plane define handle attachment sites. The important features are the images of the 1-skeleton of N , and we want a high amount of control over how these features present. We first lay out conditions required of the projection, describe a method for ensuring these conditions are met, and then turn the method into an algorithm. We do all of this before forming the base 4-manifold so that the boundary components of W contain the desired handle attachment sites.

Our subdivision of N is obtained by imposing four conditions on $f : N \rightarrow \mathbb{R}^2$:

1. f maps vertices to the circle, i.e. for each vertex $v \in N^0$, $f(v)$ lies on the unit circle in \mathbb{R}^2 .
2. The images of vertices are distinct, i.e. for every pair of vertices $u, v \in N^0$, $f(u) \neq f(v)$.
3. f is linear on each simplex of N and piecewise-linear on N , i.e. if $x \in \sigma$ is a point in the simplex σ with vertices v_i , then $x = \sum_i a_i v_i$ with $\sum_i a_i = 1$ and $f(x) = \sum_i a_i f(v_i)$.
4. Edge intersections are distinct, i.e. for every triple of edges $e_1, e_2, e_3 \in N^1$ that share no vertices, $f(e_1) \cap f(e_2) \neq f(e_2) \cap f(e_3)$.

We call these the *subdivision conditions* on f , and we call a map satisfying the subdivision conditions a *subdividing map*. Conditions 1 and 2 ensure that every simplex of N is mapped to the plane in standard position, where a simplex σ of N is mapped to the plane in *standard position* if every point in $f(\sigma^0)$ is essential in forming the convex hull of $f(\sigma^0)$ as shown in Figure 4.1. This, along with conditions 3 and 4, allows us to use concepts and language from normal surface theory to describe the subdivision of N in the next section.

All conditions are satisfied by fixing an odd integer k greater than or equal to the number of vertices in N , injecting the vertices of N to the k^{th} complex roots of unity in the plane, then extending linearly over the skeletons of N . The first three conditions are clearly satisfied by this procedure, and the last is satisfied by the results in [9].

Algorithm 1 takes as input the closed, orientable 3-manifold triangulation N and produces a subdividing map $f : N \rightarrow \mathbb{R}^2$. The subdividing map projects each tetrahedron to the plane in *standard position*, as shown in Figure 4.1.

	Data: A closed, orientable 3-manifold triangulation N
	Result: A subdividing map $f : N \rightarrow \mathbb{R}^2$
1	begin
2	$k =$ the smallest odd number greater than or equal to $ N^0 $
3	foreach vertex v_i in N^0 , $i = 1, \dots, N^0 $ do
4	$f(v_i) = (\cos(\frac{2\pi i}{k}), \sin(\frac{2\pi i}{k}))$
5	end
6	foreach n in $\{1, 2, 3\}$ do
7	foreach simplex σ in N^n do
8	By definition, σ is the set of convex combinations of σ^0 :
9	$\sigma = \{x \mid x = \sum_{i=0}^n a_i v_i, \sum a_i = 1, a_i \geq 0, v_i \in \sigma^0\}$
10	Define f on $x \in \sigma$ by requiring linearity over simplices:
11	$f(x) = f(\sum_{i=0}^n a_i v_i) = \sum_{i=0}^n a_i f(v_i)$
12	end
13	end
14	end

Algorithm 1: Constructing a subdividing map $f : N \rightarrow \mathbb{R}^2$

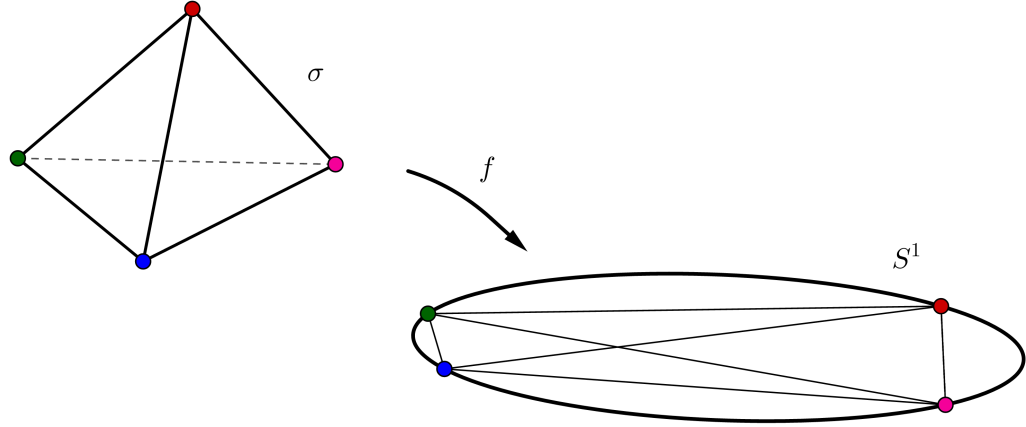


Figure 4.1: A tetrahedron σ projected to the plane in standard position through a subdividing map f . The four vertices of σ^0 map to the unit circle in the plane, thus form a convex arrangement. Four of the six edge of σ^1 map to the boundary of $f(\sigma)$, connecting $f(\sigma^0)$. The last two edges map across $f(\sigma)$, forming an intersection interior to $f(\sigma)$. Each vertex of the arrangement is essential in forming the convex hull of $f(\sigma^0)$.

4.2 Induce subdivision

The goal of subdividing N is to create and identify handle attachment sites analogous to the face, edge, and vertex blocks of Chapter 3. We use a similar technique to that found in Chapter 3, iteratively subdividing the tetrahedra of N by certain preimages of f . Tetrahedron subdivisions are compatible, i.e. tetrahedron subdivisions fit together exactly as the undivided tetrahedra do inside of N .

Let σ be a tetrahedron of N and let s be a line segment in the plane such that $s \cap f(\sigma)$ is nonempty, the endpoints of s are outside of $f(\sigma)$, and $s \cap f(\sigma)$ is a line segment in $f(\sigma)$ disjoint from any vertices or crossings of $f(\sigma)$. Figure 4.2 demonstrates the possible configurations of these line segments, and shows that their preimages inside of σ are triangles and quads. We refer to these preimages as *exterior triangles* and *exterior quads*. When a pair of these preimages intersect, the intersection is a line segment with endpoints interior to a pair of triangles of σ^2 .

For each $\sigma \in N^3$ and each edge e of N^1 such that $e \notin \sigma^1$, $f(e)$ is a line segment in the plane that is either disjoint from $f(\sigma)$ or induces an exterior triangle or quad in σ . There are two edges of σ whose preimages in σ form *interior triangles*. These are the preimages of the edges of σ that map through f across $f(\sigma)$ as in Figure 4.1, and we refer to these edges as *interior edges*. The three edges of the interior triangle

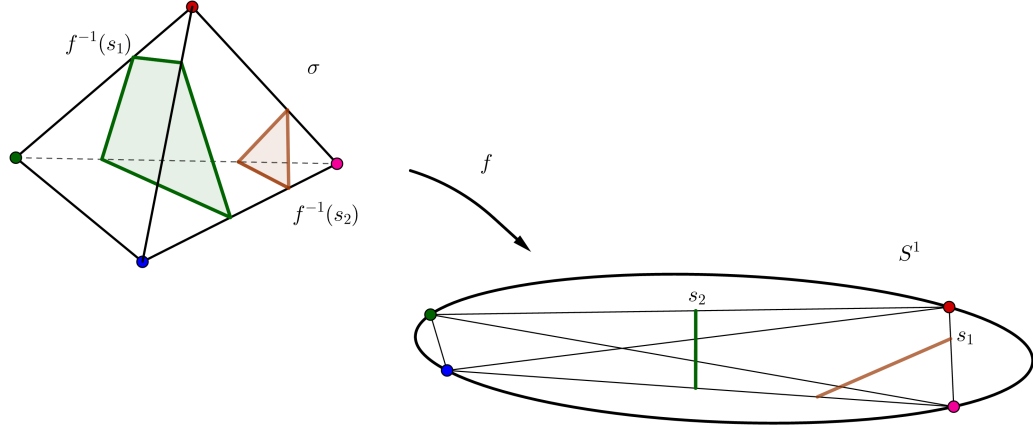


Figure 4.2: **A tetrahedron σ in standard position, intersecting edges, and preimage triangles and quads.** An intersecting edge separates the vertices of σ . If one is separated from the other three, its preimage is a triangle. If the vertices are separated into two pairs of two, the preimage is a quad.

induced by e are e itself along with a pair of edges that bisect the triangles of σ not containing e as an edge. The three vertices of the interior triangle induced by e are the two vertices of σ that are the endpoints of e along with a third vertex located in the edge of σ opposite e . Figure 4.3 shows one interior triangle along with its possible intersections with exterior triangles and quads. The interior triangles of σ always intersect in a line segment with endpoints inside of the interior edges of σ , shown in Figure 4.4

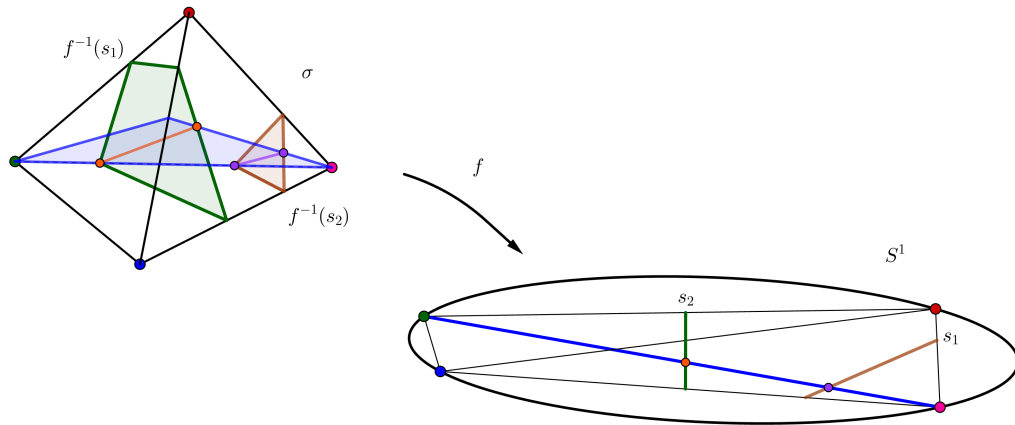


Figure 4.3: **A tetrahedron σ in standard position, one interior triangle, one exterior triangle, and one exterior quad.** There are two special preimage triangles in σ , called *interior triangles*, that occur as the preimages of the edges of σ that map through f across $f(\sigma)$ as in Figure 4.1.

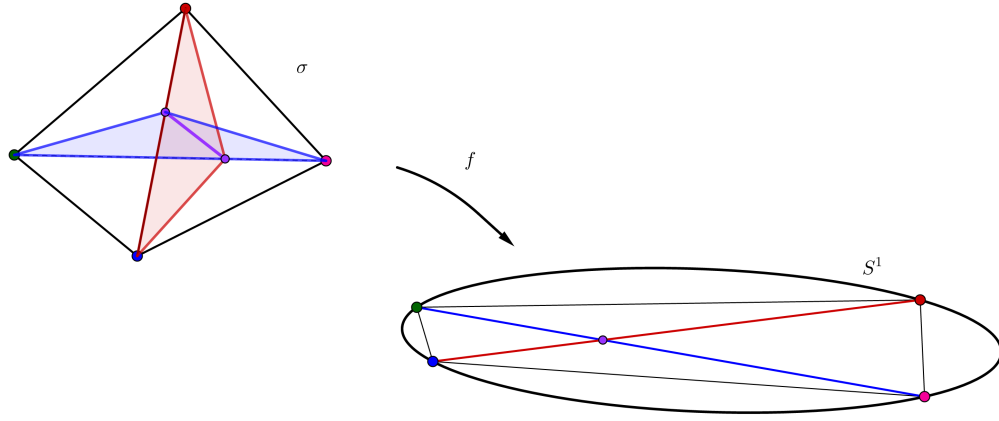


Figure 4.4: **A tetrahedron σ in standard position with both interior triangles.** As in Figure 4.3, but displaying both interior triangles.

Recall that the goal of this subdivision is to identify combinatorial analogues for the face, edge, and vertex blocks of Chapter 3. If we were to subdivide N using the quads and triangles induced by the edges of N , such blocks are ill-defined. We amend this by introducing a set of line segments analogous to the sleeves of Section 3.2.

For each edge e of N^1 , consider $e_\varepsilon^+ = s(e + \varepsilon_e e_\perp)$ and $e_\varepsilon^- = s(e - \varepsilon_e e_\perp)$, secants in the circle that are parallel to $f(e)$ and located a small orthogonal distance away from $f(e)$. Here we are using $s(\cdot)$ as a function that extends and trims line segments in the plane into secants in the circle. We require that, for each $e \in N^1$, ε_e is small enough that the rectangle R_e in the plane defined by e_ε^+ and e_ε^- does not fully contain g_ε^\pm for any $g \in N^1$. This requirement also ensures that the only crossings of $f(N^1)$ contained in R_e are crossings involving e . The segments e_ε^\pm for each $e \in N^1$ are called *sleeve segments*, and their preimages form exterior triangles and quads inside of the tetrahedra of N , as shown in Figure 4.5.

Take S to be the set of line segments in the plane that consists of $f(e)$ for each $e \in N^1$ along with the sleeve segments e_ε^\pm . For each tetrahedron σ of N , the triangles, quads, and intersections of $f^{-1}S \cap \sigma$ define a subdivision of σ into a cell complex. Iteration of this subdivision in Algorithm 2 across all tetrahedra of N yields a 3-dimensional cell complex M .

We subdivided N into M in order to identify analogues to the face, edge, and vertex blocks of Chapter 3. The analogous blocks are defined exactly as they were in Chapter 3 — the sleeve segments subdivide the plane into regions homeomorphic to disks, those disks are classified by whether they contain a crossing of $f(N^1)$, intersect

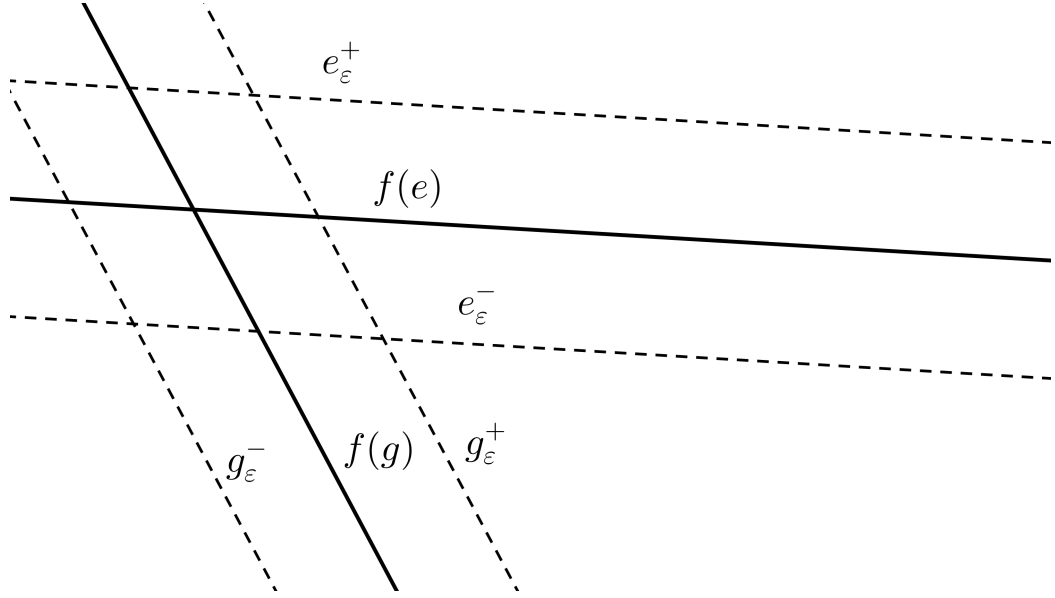


Figure 4.5: **A pair of sleeve segments in the plane.** We show a pair of edges projections $f(e)$ and $f(g)$ in the plane, along with their associated sleeve segments. Sleeve segments are necessary to ensure well-defined face, edge, and vertex block analogues in the subdivision of N .

$f(N^1)$ but do not contain a crossing, or do not intersect $f(N^1)$ at all. The preimage of a region that contains a crossing is a *combinatorial vertex block*, the preimage of a region that intersects $f(N^1)$ but does not contain a crossing is an *combinatorial edge block*, and the preimage of a region that is disjoint from $f(N^1)$ is a *combinatorial face block*. Symmetric names are used for the regions that these blocks project onto — combinatorial face (resp. edge, vertex) blocks map through f to *combinatorial face* (resp. *edge*, *vertex*) *regions*. Figure 4.6 illustrates the regions in the plane that produce such blocks. These preimages exhaust the cells of M , providing a decomposition into subcomplexes. This decomposition is not a partition — some cells are assigned to more than one block. Such an assignment happens precisely when a cell is mapped through f to the shared boundary of different combinatorial regions.

The Cartesian product of a pair of cell complexes is again a cell complex, so we form the base 4-dimensional cell-complex to which we attach handles as $M \times [0, 1]$. Every cell of $M \times [0, 1]$ is homeomorphic to a disk, so we form a 4-manifold triangulation W as a subdivision of $M \times [0, 1]$. This triangulation is obtained by inductively subdividing each cell of $M \times [0, 1]$ that is not a simplex.

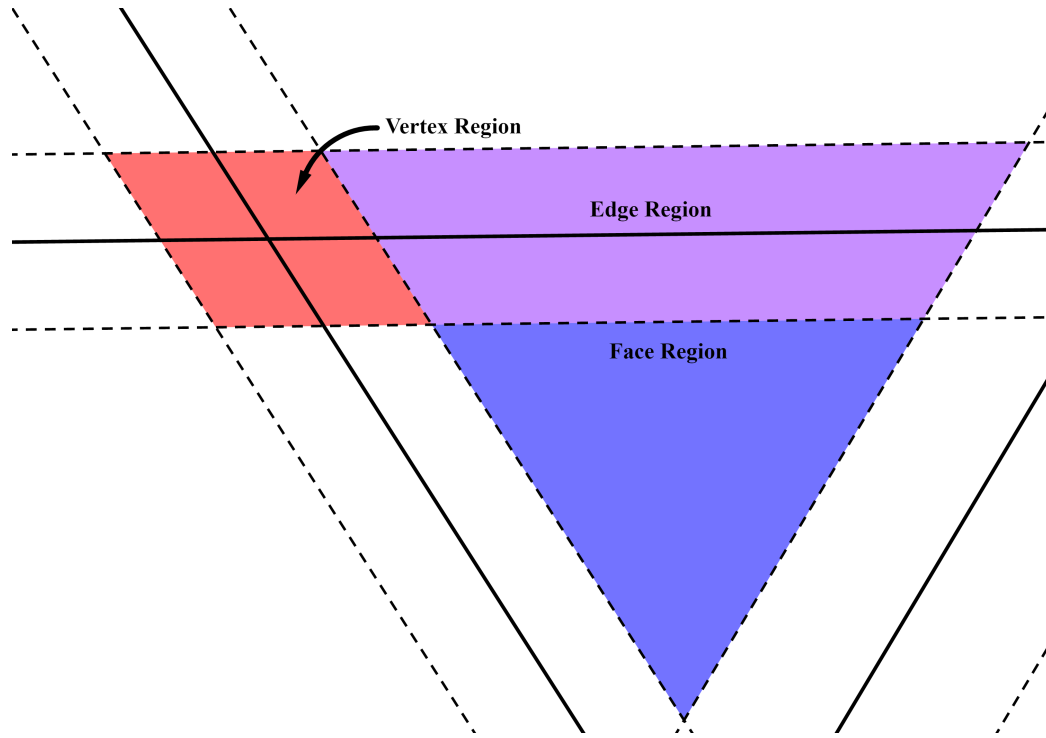


Figure 4.6: **Regions in the plane that correspond to combinatorial vertex, edge, and face block.** The sleeve segments provide the same functionality as the sleeves in Chapter 3, in that the preimages of the regions they form behave similarly to the vertex, edge, and face blocks defined in Chapter 3.

Data: A closed, orientable 3-manifold triangulation N with subdividing map $f : N \rightarrow \mathbb{R}^2$ Result: A closed, orientable 3-dimensional cell complex M	<pre> 1 begin 2 $S = \{f(e) \mid e \in N^1\} \cup \{e_\epsilon^\pm \mid e \in N^1\}$ 3 foreach tetrahedron σ of N^3 do 4 foreach segment s of S do 5 $\delta =$ the intersection of σ with $f^{-1}s$ 6 replace σ with the 3-dimensional cell complex obtained as σ subdivided by δ 7 end 8 end 9 end </pre>
--	---

Algorithm 2: Subdividing N

4.3 Attach Handles

At this point in the chapter we have constructed a 4-manifold triangulation W with two boundary components, each equivalent via subdivision to the 3-dimensional cell

complex M obtained in Section 4.2. Furthermore, the simplices of M are partitioned into subtriangulations analogous to the face, edge, and vertex blocks of Chapter 3. Explicit attachment sites are available for (4,2)–handles, so our first step is construction of a (4,2)–handle.

4.3.1 2–handles

The algorithm of this subsection takes as input a pair (T, Γ) where T is a closed solid torus triangulation and Γ is a collection disjoint parallel longitudes in the boundary of T , given as subtriangulations of ∂T . The output is a 4–disk triangulation H satisfying the following:

1. ∂H is a triangulated S^3 with a genus 1 Heegard splitting over ∂T , i.e. T is a subtriangulation of ∂H such that $\partial H \setminus \text{int}(T)$ is a solid torus.
2. For each γ_i in Γ , γ_i bounds a triangulated disk in ∂H , i.e. each γ_i is an explicit 0–framing for the (4,2)–handle attachment.

We take H to be a (4,2)–handle and attach H to W over T . Constructing the handle involves building a solid torus T' that complements T , combining T and T' over their shared boundary to build a triangulated 3–sphere, then coning that 3–sphere into the 4–disk H .

We find pairs (T, Γ) inside $M_1 \subset \partial W$, the subdivision of N induced by the subdividing map $f : N \rightarrow \mathbb{R}^2$. Let B be a combinatorial face block of M_1 . B is a 3–dimensional subtriangulation of M_1 that forms a closed solid torus, and B projects through f over an n –gon for some n . Call the n corners of $f(B)$ by c_i , $i = 1 \dots n$, and take $C = \{c_1 \dots c_n\}$. Then the $f^{-1}c_i$ are disjoint parallel triangulated longitudes of B . We take $(B, f^{-1}C)$ as our pair (T, Γ) for each combinatorial face block B of M .

For a closed solid torus T , we find a complementary torus T' , i.e. $\partial T = \partial T'$ as triangulations. We begin by investigating the boundary of T , setting $T'_0 = \partial T$. Inside T'_0 is the set of disjoint parallel longitudes Γ that are required to bound disks inside T' , so for each γ_i we attach a disk D_i with $\partial D_i = \gamma_i$ to T'_0 over γ_i . Call the result of these attachments T'_1 . Adjacent longitudes γ_i and γ_j bound an annulus A_{ij} in T'_1 , and $D_i \cup A_{ij} \cup D_j$ is a triangulated 2–sphere that we cone into a 3–disk D_{ij} . For each ij , we attach the 3–disk D_{ij} to T'_1 over $D_i \cup A_{ij} \cup D_j$ to form the closed solid torus T' .

By construction $\partial T' = \partial T$, hence the tori are complementary. The longitudinal curves of T , the γ_i , bound triangulated disks in T' thus are meridians of T' . Hence,

gluing T and T' over their shared boundary forms a 3-sphere. We then cone that 3-sphere to produce a 4-disk with an explicit (4,2)-handle structure. This is the basic structure of Algorithm 3, which we iterate over the combinatorial face blocks of $M_1 \subset \partial W$. Finally, we attach these handles to W , forming W' .

Let \mathfrak{B} be the collection of combinatorial face blocks of $M_1 \subset \partial W$. Iterating Algorithm 3 over \mathfrak{B} yields a collection of (4,2)-handles $\{H_B^2\}_{B \in \mathfrak{B}}$. The combinatorial face blocks in \mathfrak{B} are disjoint by construction, so we attach our handles in any order. We form the 4-manifold triangulation W' from W as

$$W' = W \cup \{H_B^2\}_{B \in \mathfrak{B}} / \sim,$$

where \sim is defined by $b \sim \iota(b)$, ι the identity map $H_B^2 \supset B \xrightarrow{\iota} B \subset M_1$.

	<p>Data: A pair (T, Γ) where T is a closed solid torus triangulation and Γ is a collection of disjoint parallel triangulated longitudes in ∂T</p> <p>Result: A 4-disk triangulation H_T^2 such that ∂H_T^2 is a triangulated 3-sphere with genus 1 Heegard splitting over ∂T and such that $\gamma_i \in \Gamma$ bounds a triangulated disk in $\partial H_T^2 \setminus \text{int}(T)$ for each i</p>
1	begin
2	First, we construct a complementary solid torus T' with $\partial T = \partial T'$
3	$T'_0 = \partial T$
4	foreach $\gamma_i \in \Gamma$ do
5	$D_i^2 = C(\gamma_i)$, the cone of γ_i
6	end
7	$T'_1 = T'_0 \cup \{D_i^2\} / \sim$, where \sim is induced by $\partial D_i^2 = \gamma_i \xrightarrow{\iota} \gamma_i \subset T'_0$
8	foreach adjacent pair of longitudes γ_i, γ_j from Γ do
9	A_{ij} = the annulus in T'_1 bounded by γ_i and γ_j
10	S_{ij}^2 = the triangulated 2-sphere in T'_1 that is precisely $D_i^2 \cup A_{ij} \cup D_j^2$
11	$D_{ij}^3 = C(S_{ij}^2)$, the cone of S_{ij}^2
12	end
13	$T' = T'_1 \cup \{D_{ij}^3\} / \sim$, where \sim is induced by $\partial D_{ij}^3 = S_{ij}^2 \xrightarrow{\iota} S_{ij}^2 \subset T'_1$
14	$S_T^3 = T \cup T' / \sim$, where \sim is induced by $\partial T \xrightarrow{\iota} \partial T'$
15	$H_T^2 = C(S_T^3)$, the cone of S_T^3
16	end

Algorithm 3: Constructing a (4,2)-handle

The manifold W' is formed by attaching triangulated (4,2)-handles to W over the combinatorial face blocks of M_1 . The boundary of W' consists of $M_0 \cup M'_1$, where $M'_1 = \partial W' \setminus M_0$ and M'_1 is related to M_1 via triangulated (3,2)-handle attachments to

M_1 induced by the triangulated (4,2)–handle attachments to W . We decompose M'_1 into primed combinatorial edge or vertex block subtriangulations in a manner similar to that found in Chapter 3.

Primed combinatorial edge blocks are the result of attaching triangulated (3,2)–handles over annular boundary components of combinatorial edge blocks. These (3,2)–handles are the triangulated 3-disks D_{ij}^3 formed on Line 11 of Algorithm 3, and their attaching regions are the annuli of combinatorial edge blocks that project through f over edge-face region boundaries.

Let E be a combinatorial edge block. Then E is the product of an orientable surface with an interval, i.e. $E = \Sigma \times [0, 1]$, where Σ is S^2 minus some number of disjoint open balls. The annuli $\partial\Sigma \times [0, 1]$ map through f to edge-face region boundaries, hence these are the attaching sites of (3,2)–handles. Primed combinatorial edge blocks are constructed by performing all such (3,2)–handle attachments, thus each primed combinatorial edge block is a triangulated $S^2 \times [0, 1]$.

Differing slightly from Chapter 3, this exhausts the new cells of M'_1 introduced by 2–handle attachment. This is due to the different shape of combinatorial vertex regions as compared to the vertex regions of Chapter 3. In Chapter 3 vertex regions were octagonal and shared edge boundaries with face regions. Here, combinatorial vertex regions are quadrilateral and share point boundaries with combinatorial face regions. This point boundary is also shared by a pair of combinatorial edge regions.

Let x be a vertex-face-edge-edge boundary. Then $f^{-1}(x) = \{\gamma^i\}$ is a collection of triangulated circles, and each γ^i is a longitude of a toroidal combinatorial face block in M_1 that projects over the face region whose boundary contains x . Thus, every γ^i has been filled by a 2–disc constructed on Line 5 of Algorithm 3. Each of these new disks has been assigned to two primed combinatorial edge blocks, but we will also assign them to the primed vertex block that contains γ^i .

This means that each primed combinatorial vertex block is now equivalent to a triangulated (3,2)–handlebody. Let V be a combinatorial vertex block and V' be V primed. Considering each new disc in V' to be a flattened (3,2)–handle, we conclude that V' is a (3,2)–handlebody using the argument found in Theorem 3.4.1. The attaching spheres of (3,2)–handles transversely intersect the belt spheres of the (3,1)–handles at most once, each belt sphere intersects at least one attaching sphere and vice versa, and the boundary of V' is a disjoint collection of 2–spheres, thus V' is a (3,2)–handlebody.

4.3.2 3–handles

We now construct (4,3)–handles to attach over our primed combinatorial edge blocks. Let E' be such a block. Then $\partial E'$ is a disjoint pair of triangulated 2–spheres. We form a 4–disk containing E' in its boundary by a double coning method on E' : we first cone the spherical boundary components of E' to form a pair of triangulated 3–disks, glue these 3–disks to E' to form a 3–sphere, then cone the 3–sphere to obtain a 4–disk. This idea is identical to that found in Section 3.4.2 and is formalized in Algorithm 4. Finally, we attach (4,3)–handles built using Algorithm 4 to W' over primed combinatorial edge blocks.

Let \mathfrak{E}' be the collection of primed combinatorial edge blocks of $M'_1 \subset \partial W'$. Iterating Algorithm 4 over \mathfrak{E}' yields a collection of (4,3)–handles $\{H_{E'}^3\}_{E' \in \mathfrak{E}'}$. The primed combinatorial edge blocks in \mathfrak{E}' intersect only in discs that are also shared by primed combinatorial vertex blocks and these discs are invariant under the (4,3)–handle attachment so we attach our handles in any order. We form the 4–manifold triangulation W'' from W' as

$$W'' = W' \cup \{H_{E'}^3\}_{E' \in \mathfrak{E}'} / \sim,$$

where \sim is defined by $e \sim \iota(e)$, ι the identity map $H_{E'}^3 \supset E' \xrightarrow{\iota} E' \subset M'_1$.

Data: E' , a triangulated $S^2 \times [0, 1]$
Result: A 4–disk triangulation $H_{E'}^3$ such that $\partial H_{E'}^3$ is a triangulated 3–sphere containing E' as a subtriangulation

```

1 begin
2   First, we attach 3–disks to  $E'$  over its two 2–sphere boundary components
3   foreach boundary sphere  $S_i^2 \in \partial E'$  do
4      $C(S_i^2)$  = the cone of  $S_i^2$ 
5     Attach  $C(S_i^2)$  to  $\partial E'$  over  $S_i^2 \in \partial E'$ 
6   end
7   The result of the above attachments is the 3–sphere  $S_{E'}^3$ 
8   Then  $H_{E'}^3 = C(S_{E'}^3)$ 
9 end
```

Algorithm 4: Constructing a 3–handle

The manifold W'' is formed by attaching triangulated (4,3)–handles to W' over the primed combinatorial edge blocks of M'_1 . The boundary of W'' consists of $M_0 \cup M''_1$, where $M''_1 = \partial W'' \setminus M_0$ and M''_1 is related to M'_1 via triangulated (3,3)–handle

attachments to M'_1 induced by the triangulated (4,3)–handle attachments to W' . These (3,3)–handle attachments turn primed combinatorial vertex blocks into double primed combinatorial vertex blocks. A primed combinatorial vertex block is a (3,2)–handlebody, so a double primed combinatorial vertex block is a (3,2)–handlebody with each S^2 boundary component filled in with a (3,3)–handle, thus each double primed combinatorial vertex block is a triangulated S^3 .

4.3.3 4–handles

We now construct (4,4)–handles to attach over our double primed combinatorial vertex blocks. Let V'' be such a block. Then V'' is a triangulated S^3 , so a (4,4)–handle structure that can be attached over V'' is constructed by coning V'' . These handles are attached to W'' to form a triangulated 4–manifold whose only boundary component is M_0 .

Let \mathfrak{V}'' be the collection of double primed combinatorial vertex blocks of $M''_1 \subset \partial W''$. Coning each element of \mathfrak{V}'' yields a collection of (4,4)–handles $\{H^4_{V''}\}_{V'' \in \mathfrak{V}''}$. The double primed combinatorial vertex blocks in \mathfrak{V}'' are disjoint, so we attach our handles in any order. We form the 4–manifold triangulation W''' from W'' as

$$W''' = W'' \cup \{H^4_{V''}\}_{V'' \in \mathfrak{V}''} / \sim,$$

where \sim is defined by $v \sim \iota(v)$, ι the identity map $H^4_{V''} \supset V'' \xrightarrow{\iota} V'' \subset M''_1$.

The triangulated 4–manifold W''' has only one boundary component: M_0 . By construction, M_0 is equivalent to the original input 3–manifold triangulation N by subdivision of N , hence W''' is a triangulated 4–manifold with boundary N , as desired.

Chapter 5

Discussion

The main chapters of this thesis serve different roles in the greater mathematical ecosystem. It is evident from the discussion in Section 2.2 of [3] that the ideas behind the constructive proof in Chapter 3 is not itself novel, but the details had yet to be published. Chapter 3 fills a hole in the current literature, whereas the contents of Chapter 4 are entirely new, serving as a solid foundation for future research in computational topology.

The immediate next step from creation of the algorithm is an implementation for a topology software project such as Regina. Such an implementation furthers progress toward algorithmic computation of the Rokhlin invariant for 3-manifolds and serves as another tool in generating 4-manifold censuses. In its current form, the construction algorithm guarantees no topological features of the constructed 4-manifold save that its boundary is the given input 3-manifold. Lucrative avenues of exploration would therefore include an investigation into invariants (e.g. the fundamental group) or constructs (e.g. spin structures) on the constructed manifold.

This work was initially an attempt to adapt the Turaev Reconstruction Theorem as an algorithm on 3-manifolds triangulations. The theorem was introduced by Turaev [14] and is also covered by Costantino [2]. The algorithm would build on the process outlined in Chapter 4 of Costantino and Thurston [3], where a quadratic bound is achieved for the number of simplices needed to triangulate a 4-manifold constructed using the reconstruction theorem.

Such an adaptation necessarily passes through the shadow realm. The shadows explored in [14] are 2-complexes with strict structural restrictions imposed upon them. In the reconstruction theorem, a shadow serves as a set of instructions for a handle decomposition of the desired 4-manifold. Each 0-cell prescribes a $(4,0)$ -handle, each

1-cell a $(4,1)$ -handle, and each 2-cell a $(4,2)$ -handle. The resulting 4-manifold W has boundary exactly the original 3-manifold M . Two major obstructions eventually caused this adaptation attempt to be scrapped:

1. Precisely defining $(4,2)$ -handle attachment sites in this process is hard.
2. The fact that $\partial W = M$ at the end of this process is not obvious and requires a deep examination of shadows (briefly, $\partial W = M$ because M and W have the same shadow).

Instead, the results of this work were obtained by turning the reconstruction theorem on its head: we begin by making the precise definition of $(4,2)$ -handle attachment sites as simple as possible. Once $(4,2)$ -handles have been attached, attachment of $(4,3)$ - and $(4,4)$ -handles is straightforward. This method is dual to the Turaev Reconstruction Theorem in its approach and handle indexing ($((n, \lambda)$ - and $(n, n - \lambda)$ -handles are identical, just attached over complementary portions of the handle's boundary), but the goals are different. Turaev's work is focused on studying the topology of the shadows themselves, where our ultimate goal is algorithmic construction of 4-manifolds with prescribed boundary.

Beyond its raw results, this research is a demonstration of adapting an existence proof into a constructive proof. More adaptations of existence proofs should not be surprising as the bounds of scientific computability are pushed.

Bibliography

- [1] Benjamin Burton, Ryan Budney, William Pettersson, et al. Regina: Software for low-dimensional topology. <http://regina.sourceforge.net/>, 1999–2019.
- [2] Francesco Costantino. A short introduction to shadows of 4-manifolds. <https://arxiv.org/abs/math/0405582/>, 2005.
- [3] Francesco Costantino and Dylan Thurston. 3-manifolds efficiently bound 4-manifolds. *Journal of Topology*, (3) 1, 2008.
- [4] Marc Culler, Nathan M. Dunfield, and Jeffrey R. Weeks. Snappy, a computer program for studying the geometry and topology of 3-manifolds, 2017.
- [5] Robert Gompf and András Stipsicz. *4-Manifolds and Kirby Calculus*. American Mathematical Society, 1999.
- [6] John M. Lee. *Introduction to Smooth Manifolds*. Springer, 2000.
- [7] Harold Levine. Elimination of cusps. *Topology*, 3(2):263–296, 1965.
- [8] W.B.R. Lickorish. A representation of orientable combinatorial 3-manifolds. *Annals of Mathematics*, 73(3), 1962.
- [9] Bjorn Poonen and Michael Rubinstein. The number of intersection points made by the diagonals of a regular polygon. *SIAM Journal on Discrete Mathematics*, (1) 11:135–156, 1998.
- [10] Colin Rourke. A new proof that Ω_3 is zero. *J. London Math. Soc.*, (2) 31:373–376, 1985.
- [11] Osamu Saeki. *Topology of Singular Fibers of Differentiable Maps*. Lecture Notes in Mathematics 1854. Springer, 2004.

- [12] Saul Schleimer. Waldhausen's theorem. *Geometry & Topology Monographs*, 12:299–317, 2007.
- [13] René Thom. Quelques propriétés globales des variétés différentiables. *Commentarii Mathematici Helvetici*, 38:17–86, 1954.
- [14] Vladimir Turaev. Topology of shadows, 1991. Preprint.
- [15] Shmuel Weinberger. *The topological classification of stratified spaces*. Chicago, 1994.